Spring 2014

MICROSTRUCTURAL INDICATORS OF TRANSITION MECHANISMS IN TIME-DEPENDENT FATIGUE CRACK GROWTH IN NICKEL BASE SUPERALLOYS

Ann Elizabeth Heeter
Purdue University

Graduate School ETD Form 9
(Revised 01/14)

PURDUE UNIVERSITY
GRADUATE SCHOOL
Thesis/Dissertation Acceptance

This is to certify that the thesis/dissertation prepared

By Ann Elizabeth Heeter

Entitled
MICROSTRUCTURAL INDICATORS OF TRANSITION MECHANISMS IN TIME-DEPENDENT FATIGUE CRACK GROWTH IN NICKEL BASE SUPERALLOYS

For the degree of Master of Science in Material Science Engineering

Is approved by the final examining committee:

David Johnson

Matthew Krane

Rodney Trice

Kevin Trumble

To the best of my knowledge and as understood by the student in the *Thesis/Dissertation Agreement. Publication Delay, and Certification/Disclaimer (Graduate School Form 32)*, this thesis/dissertation adheres to the provisions of Purdue University's "Policy on Integrity in Research" and the use of copyrighted material.

David Johnson

Approved by Major Professor(s): _____

_____

Approved by: David Bahr 04/25/2014

Head of the Department Graduate Program Date

MICROSTRUCTURAL INDICATORS OF TRANSITION MECHANISMS IN TIME-DEPENDENT FATIGUE CRACK GROWTH IN NICKEL BASE SUPERALLOYS

A Thesis

Submitted to the Faculty

of

Purdue University

by

Ann E Heeter

In Partial Fulfillment of the

Requirements for the Degree

of

Master of Science in Material Science Engineering

May 2014

Purdue University

West Lafayette, Indiana

For my family and friends, your support has been invaluable as I pursue my aspirations.

ACKNOWLEDGEMENTS

I would like to first acknowledge David Mills as my Rolls-Royce thesis advisor. It was his guidance that inspired this research program and his dedication that helped ensure that the research progressed. I appreciate all of his assistance and I look forward to future research endeavors.

I would also like to acknowledge Professor David Johnson for his support of my thesis research. He has been truly supportive of my dedication to complete my research while maintaining my professional commitments. Professor Johnson embodies Purdue's commitment to research and he is a true asset to the university.

TABLE OF CONTENTS

Page

Page

LIST OF TABLES

LIST OF FIGURES

Figure Page

Figure Page

Figure Page

Figure Page

LIST OF ABBREVIATIONS

CTOD: Crack Tip Opening Displacement

DCPD: Direct Current Potential Drop

DOE: Design of Experiments

DTT: Dwell Transition Temperature

EDM: Electro-Discharge Machining

FEA: Finite Element Analysis

Kb: Surface flaw type crack growth specimen

LEFM: Linear Elastic Fracture Mechanics

SEI: Secondary Electron Imaging

SEM: Scanning Electron Microscope

ABSTRACT

Heeter, Ann E. M.S.M.S.E., Purdue University, May 2014. Microstructural Indicators of Transition Mechanisms in Time-Dependent Fatigue Crack Growth in Nickel Base Superalloys. Major Professor: David Johnson.

Gas turbine engines are an important part of power generation in modern society, especially in the field of aerospace. Aerospace engines are design to last approximately 30 years and the engine components must be designed to survive for the life of the engine or to be replaced at regular intervals to ensure consumer safety. Fatigue crack growth analysis is a vital component of design for an aerospace component. Crack growth modeling and design methods date back to an origin around 1950 with a high rate of accuracy. The new generation of aerospace engines is designed to be efficient as possible and require higher operating temperatures than ever seen before in previous generations. These higher temperatures place more stringent requirements on the material crack growth performance under creep and time dependent conditions. Typically the types of components which are subject to these requirements are rotating disk components which are made from advanced materials such as nickel base superalloys.

Traditionally crack growth models have looked at high temperature crack growth purely as a function of temperature and assumed that all crack growth was either controlled by a cycle dependent or time dependent mechanism. This new analysis is trying to evaluate the transition between cycle dependent and time dependent mechanism and the microstructural markers that characterize this transitional behavior. The physical indications include both the fracture surface morphology as well as the shape of the crack front. The research will evaluate whether crack tunneling occurs and

whether it consistently predicts a transition from cycle-dependent crack growth to time-dependent crack growth. The study is part of a larger research program trying to include the effects of geometry, mission profile and environmental effects, in addition to temperature effects, as a part of the overall crack growth system. The outcome will provide evidence for various transition types and correlate those physical attributes back to the material mechanisms to improve predictive modeling capability.

CHAPTER 1. INTRODUCTION

1.1 Purpose

The goal of this project is to use a combination of predicative modeling and experimental testing to improve the fatigue crack growth life assessment method for high temperature aerospace applications. Rotating disk components in aerospace engines are required to be capable of lasting for long periods of time at high temperatures and high loading conditions. The engine mission profile may include several harsh conditions for a material including take-off, cruise, and landing. An example of the loading associated with an airplane flight is shown in Figure 1.1.

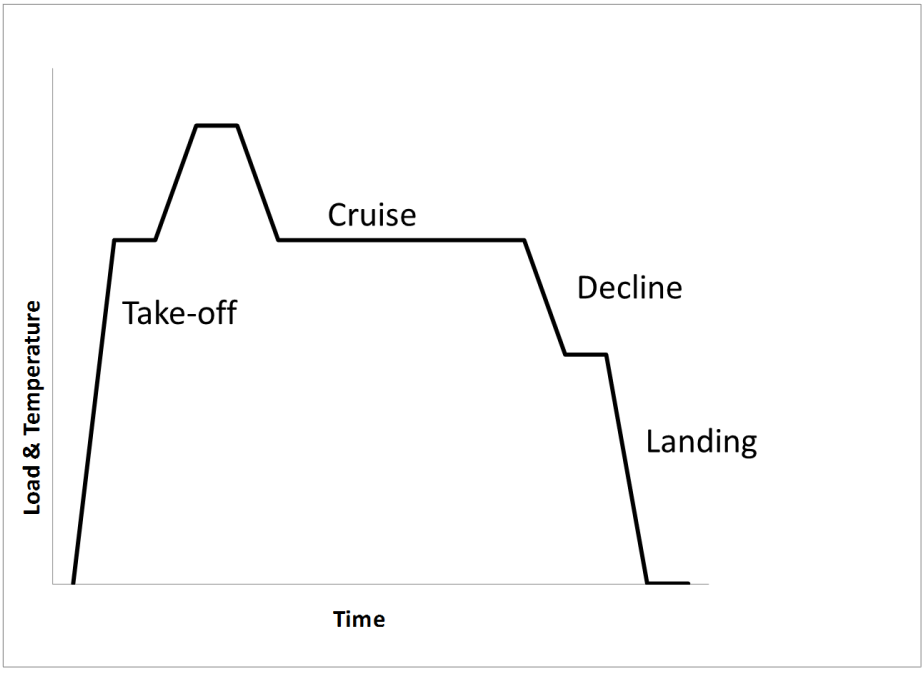

Figure 1.1 Aerospace engine mission profile showing flight load levels on engine components

Historically, the take-off and landing condition are the most critical based on the high stresses and thermal gradients, respectively. The cruise condition is gaining increasing importance as the temperatures increase for this segment of the mission.

The fatigue capability of the disk components can be scaled from low temperature to high temperature applications. After initiation, though, the crack growth experiences a mechanism shift at high temperatures which can be more difficult to predict. In order to predict how long these components can operate in the engine before requiring replacement or the "life" of a component, models must be produced which are referred to as "disk life assessment methods." Most life assessment methods rely on a combination of fatigue life and crack growth life to determine the total life of a component. These assessments are produced through a mathematical models and physical validation via testing.

The current fatigue crack growth models are split between cycle-dependent and time-dependent crack growth. Cycle-dependent crack growth assumes that the component is operating in a lower temperature and low stress regimes, while time-dependent crack growth is applied in a high temperature and high stress regimes. Two different types of are used to predict crack growth behavior for each regime. A visual representation of the two crack growth regimes is shown below.

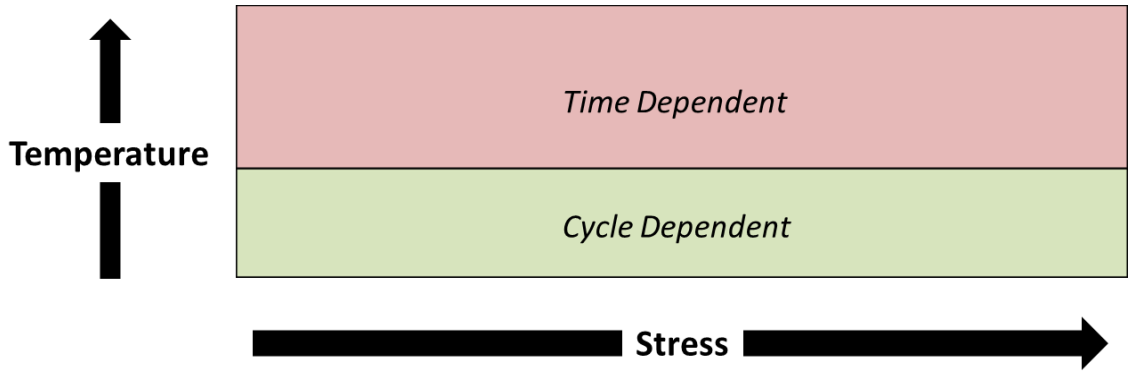

Figure 1.2 Illustration of the transition from cycle-dependent to time-dependent crack growth

This simplistic approach makes it relatively easy to determine which crack growth method to use; however, it may be too conservative for those low stress/ high temperature and high stress/ low temperature conditions. This investigation is part of a larger research program designed to create a new modeling method for those intermediate conditions which may not be fully cycle dependent of fully time dependent. This portion of the work will focus on the data and microstructural indicators of the intermediate condition or transition state.

The larger research program established a Design of Experiments (DOE) to target a range of conditions to model and test the predicted response. The outer bounds of the model were those conditions which were expected to be time dependent and those which were expected to be cycle dependent. The potential transition conditions were targeted for the intermediate region with small increments established at different test parameters to try and determine which conditions will cause transition. The theory is that test parameters such as load sequence, geometry, dwell time at high temperatures, and creep effects may determine whether a condition will transition or not. A visual representation of the DOE is shown in Figure 1.3.

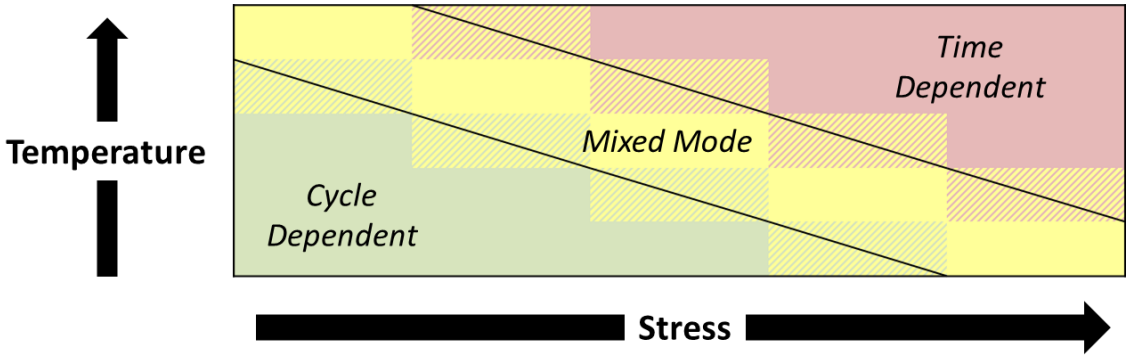

Figure 1.3 An example of the mechanism map configuration

Finite Element Analysis (FEA) was performed on targeted conditions and then validation testing was performed using crack growth specimens to ensure accuracy. This specific publication will analyze the test data produced and physical appearance of the test specimens to categorize the evidence of transition.

1.2 Material

Based on these engine operating conditions, the disk components in these aerospace engines are typically made from nickel-base superalloys for their temperature and strength capability. All three materials have a face centered cubic crystal structure. The strength is partially attributed to precipitation hardening, the γ' precipitates act as a barrier to dislocation motion. The precipitates act to block dislocation motion and resist crack growth. Nickel base superalloys also have a high chromium content which makes them oxidation and corrosion resistant.

Three nickel-base superalloys were selected for this research program: Udimet 720 (U-720), Inconel 718 (IN-718) and Waspaloy. These materials were chosen for their popularity in the aerospace industry and their high temperature capability. All three alloys were processed via hot die forging process and heat treated per the material specifications. This indicates that all three materials will have a slightly different microstructure and grain size. U-720 has the best high temperature capability with limited creep effects at high temperature and the highest room temperature yield strength. Creep resistance is the material ability to withstand creep deformation at an elevated temperature and constant applied load. Waspaloy is the intermediate alloy which has performance characteristics that fall between U-720 and IN-718 in terms of creep capability. The Waspaloy material also has the lowest yield strength. IN-718, on the opposite end of the spectrum, is the least temperature capable and the most susceptible to creep effects. It has an intermediate level yield strength in comparison to the other two materials.

While all three materials have slightly different characteristics, they were also intentionally selected based on their similarity. All three alloys are expected to have a similar type of transition from time-dependent to cycle-dependent crack growth. This research seeks to categorize this sub-set of alloys and create the potential to use the results to predict the behavior of other alloy groups in future research.

1.3 Scope and Confinements

This summary will primarily focus on the experimental test program and material response to test conditions. The thesis will provide a background on crack growth theory that contributes to this response and documents the previous work that leads up to this research. The theoretical models were developed with the core information from these theories and the test conditions were selected in order to validate the transition points which can occur between competing mechanisms. The theoretical models will not be explicitly discussed in this thesis, but more information about the models will be published in a recently submitted patent application (Mills, 2014).

1.4 Outline of Report

This report will start with a summary of time dependent and environmentally driven fatigue crack growth mechanisms in Chapter 2. The background section will also look at basic fatigue crack growth concepts that are common to all materials and conditions. Chapter 3 will discuss how these theoretical concepts are translated into a research program and experimental testing. Chapter 4 will provide an overview of the experimental methods, the parameters that were tested, and the laboratory analysis. Chapter 5 will contain the test results and a summary of the physical material response. Chapter 6 will discuss the material response compared to the theoretical mechanisms. Chapter 7 will summarize the conclusions of this work and recommend future testing that could be performed to improve the theories posited here.

CHAPTER 2. BACKGROUND

2.1 Time Dependent Crack Growth

Time dependent fatigue crack growth is a temperature activated fatigue crack growth mechanism which results from the material being held at a maximum load at an elevated temperature. The dwell period simulates the high temperature cruise condition in an aerospace engine. Materials which are susceptible to this condition typically have a Dwell Transition Temperature (DTT) or the threshold temperature above which the influence of dwell must be included in the crack propagation predictions. The dwell transition temperature is an experimentally determined value which indicates when the switch from cycle dependent to time dependent crack growth should occur. To date, there is no universally accepted standard test to determine this value. Therefore the DTT is typically produced by individual groups who use time dependent crack growth modeling. The DTT is typically near the temperature range where creep and oxygen diffusion start to occur for a given alloy. Therefore, the DTT will be different for each alloy and must be experimentally determined. Material which is not affected by the dwell condition or is below the DTT undergoes cycle dependent crack growth. The intermediate condition is crack growth which falls in between cycle dependent and time dependent crack growth which is considered mixed mode crack growth. Mixed mode crack growth may display characteristics of both types of crack growth. This could be visible in the crack growth rate or on the physical appearance of the material.

Typically cycle dependent crack growth propagates along a transgranular path. Time dependent crack propagation propagates along an intergranular path. Mixed mode crack growth may include both transgranular and intergranular crack propagation. Time dependent crack growth is heavily dependent on the crack growth environment. This can include several parameters in addition to temperature such as length of dwell time, oxygen diffusion, partial pressure, and microstructural effects of material. The grain orientation relative to the loading direction influences the dislocation alignment and can strongly affect fracture progression (Prakash, Walsh, Maclachan, & Kcrunsky, 2009). During testing to simulate time-dependent crack growth, a dwell period is imposed at the maximum load in the waveform force transition to occur. The fracture surface will only switch to intergranular crack growth if the dwell is applied under high temperature conditions.

VanStone et al. highlighted the effect of time dependent crack growth in turbine disk alloys. An experimental program was performed to validate a mathematical model of crack growth in a time dependent regime. The oxygen environment is the most damaging for crack growth. However, the environmental conditions are less significant at high frequency testing in comparison to low frequency testing. There are several factors which dictate how time dependent crack growth occurs in different alloys: grain size, ultimate tensile strength, and chromium content. The chromium content helps protect superalloy materials from high temperature oxygen diffusion. Of the three types of crack growth curve fits, time dependent crack growth is typically modeled using hyperbolic sine or sigmoidal curve fit. One of the models that VanStone et al. provided to account for time dependent crack growth is the superposition model. The total crack growth is the sum of the cyclic crack growth and the time dependent crack growth per the equation below (VanStone, Gooden, & Krueger, 1988).

Equation 1 VanStone Superposition Model

$$\frac{da}{dN} = \left(\frac{da}{dN}\right)_C + \Delta a$$

da/dN = total crack growth rate

$(da/dN)_C$ = cyclic crack growth rate

$\Delta a = \left(\frac{da}{dN}\right)_{Time}$ = time dependent crack growth rate

The superposition model assumes that the crack growth rate results from cycle dependent and time dependent results can be used in concert to accurately predict the total crack growth of a system (VanStone, Gooden, & Krueger, 1988).

Time dependent crack growth can have a dwell period at either the maximum applied load or the minimum applied load. In a study by Bache et al., dwell periods were applied at both the maximum and minimum load condition to compare the resulting crack growth rates. All specimens were exposed at elevated temperatures to induced oxidation effects prior to testing. There was no change in the fatigue life based on the differences in dwell period; however, there were some indications of environmental damage from the pre-exposure period affected the crack growth rate (Bache, Jones, Drew, Hardy, & Fox, 2009). In this analysis, no thermal exposure is being performed prior to testing and the dwell period will be applied at the maximum load level which is assumed to be the most conservative way to establish a life assessment program.

2.1.1 Microstructural Mechanisms

There are several different types of microstructural mechanisms which can either act to promote the transition from transgranular to intergranular crack propagation. These are defined as either intrinsic or extrinsic mechanisms. Intrinsic mechanisms are those factors which are inherent to the material that influence the crack growth behavior of the alloy and operate ahead of the crack tip. Intrinsic

mechanisms are those factors present in the material such as the predisposition for dislocation motion or the atomic bonding which can create micro-cracks or voids. Extrinsic mechanisms are those factors which exist in the environment around the alloy or the type of loading applied to the alloy which influences the crack growth behavior of the material. Extrinsic mechanisms typically operate behind the crack tip and influence the driving force for crack propagation. Some crack growth models try to account for this factors as a part of a random anomaly distribution based on statistical data on various materials. Extrinsic mechanisms are typically shielding mechanisms which can alter the inelastic zones around the crack wake (Ritchie, 1999). Intrinsic mechanism can cause crack initiation in a material while extrinsic mechanisms can only expedite crack growth after initiation. Ductile materials are toughened through intrinsic mechanisms, while brittle materials are toughened through extrinsic mechanisms. The level of surface roughness also has a large impact on the amount of crack closure at near threshold levels (Ritchie, 1999).

The overall takeaway from these theories suggests that there are competing mechanisms which occur in an air environment, some of which retard crack growth and some of which accelerate crack growth. A visual representation of the more common mechanisms relative to the crack tip is shown in Figure 2.1.

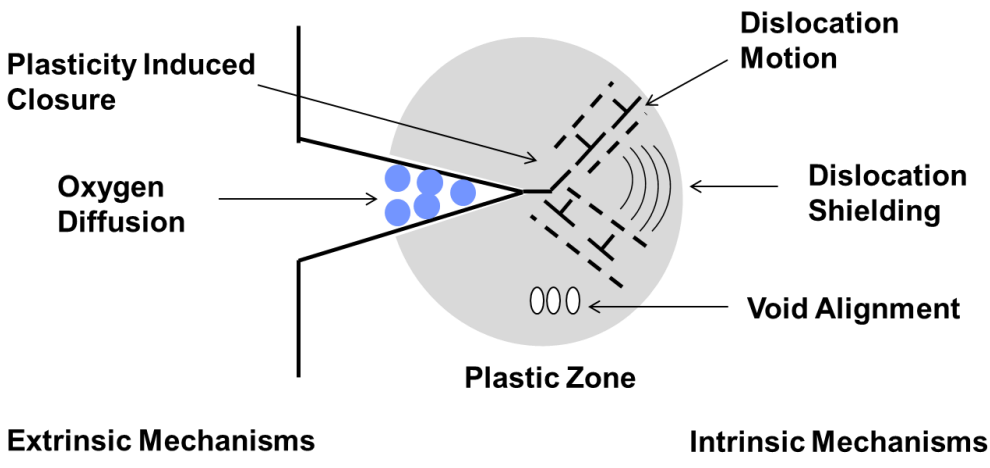

Figure 2.1 Schematic of the various microstructural mechanisms relative to the crack and the adjacent plastic zone

There are debates on which mechanism has the greatest driving force. This research will seek to demonstrate that there are a large variety of test parameters which can affect the impact of the competing mechanisms. Some of these parameters include geometry, material composition, temperature, load, and dwell.

2.1.1.1 Material Interactions with Mechanisms

Nickel base superalloys have two major microstructural features that contribute to the material properties. The first is the gamma prime (γ') precipitates which contribute to the precipitation strengthening in the material and prevent overall dislocation motion. The size of the γ' particles is important because the overall volume fraction determines the relative ease of dislocation motion in the material. The second is the presence of carbides which form from some of the more common compositional elements such as chromium, molybdenum, tungsten, niobium, tantalum and titanium. The carbides improve the creep properties of nickel-base superalloys and act to strengthen the grain boundaries of the material (Reed R. C., 2006).

The Hall-Petch Relationship is a correlation between material grain size and strength of the corresponding material. The relationship between material yield strength and the average grain size is shown in Equation 2.

Equation 2 Hall-Petch Equation

$$\sigma_y = \sigma_0 + k_y d^{-1/2}$$

In this model, σ_y is the material yield strength, d is the average grain size, σ_0 and k_y are material specific constants (Askeland & Fulay, 2005). The Hall-Petch Relationship is referenced as part of the motivation for evaluating three different alloys with slightly different grain sizes. Typically grain size is connected to the effect on monotonic stress-strain behavior. Morrison et al attempted to make a connection between the grain size and cyclic stress-strain behavior in nickel based materials. Slip band localization causes cyclic strain hardening which is evident in the hysteresis loops and grain size has a direct link to the amount of strain localization. In their

experimental study, both fine and coarse grain Nickel-270 alloy were evaluated under cycle deformation at room temperature. The results demonstrated that both the fine and coarse grain version of the alloy showed a similar amount of cyclic hardening. However, fine grain material reached a higher level of strain saturation before the coarse grain material. This suggests that transgranular crack propagation is expected for the fine grain material (Morrison, Chopra, & Jones, 1991). The microstructure and grain size of the material will be used to evaluate whether a material will transition from cycle-dependent to time-dependent crack growth.

2.1.1.2 Environmental Interactions

As mentioned above, the environment around a material can strongly influence the crack growth mechanism and the crack growth rate. For both cycle dependent and time dependent crack growth, the material crack growth behavior changes dramatically between alloys tested in a vacuum environment compared to alloys tested in air. Those alloys which have been tested in vacuum consistently display a transgranular crack progression regardless of dwell period, while those tested in air under the same conditions can display an intergranular crack progression at elevated temperatures.

The period of time when a fracture is growing within the cross section of a material can simulate a vacuum-type environment while the crack moves through the specimen interior. Therefore, some specimens show signs of transgranular crack growth until the crack breaks the surface of the material and exposes the fracture surface to an air environment. Oxygen present in an air environment diffuses into the material grain boundaries causing an embrittling effect which forces the crack onto an intergranular path. More homogeneous microstructures lead to more uniform crack growth rates under these mechanisms, whereas any deviations in microstructure can alter the crack growth rate (Caton & Jha, 2010). At high temperature, the diffusion process is intuitively faster than in a cooler temperature range.

Oxygen diffusion occurs in two stages, the first stage is oxide layer formation on the crack surface and the second stage is diffusion into the area ahead of the crack tip. Oxides typically move along grain boundaries as the lowest energy configuration. An illustration of the oxygen diffusion process is shown in the figure below.

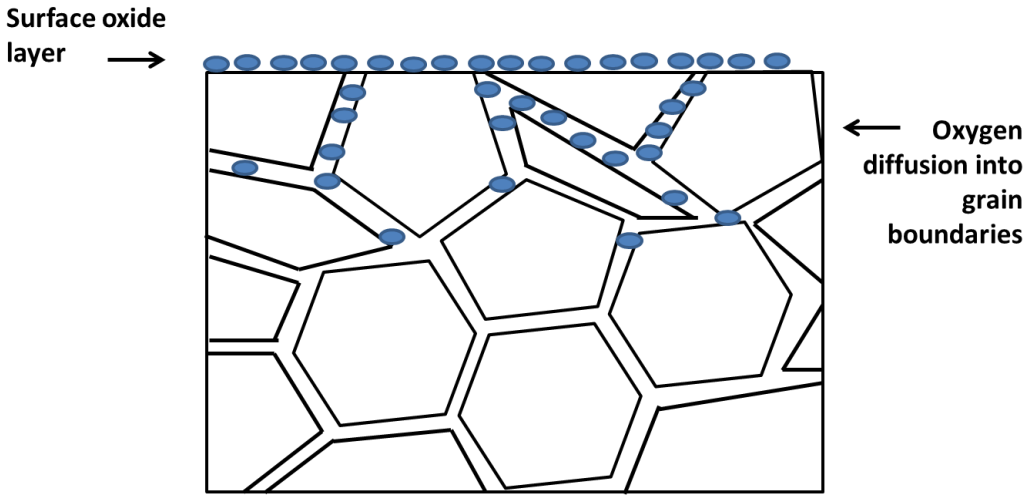

Figure 2.2 An illustration of the oxygen diffusion process on a microstructural level

The amount of diffusion depends on the partial pressure surrounding the crack surface. Additionally, higher levels of chromium were found along the grain boundary diffusion path, which forms a protective layer and prevents further oxidation (Zheng & Ghonem, Part I, 1991).The partial pressure of the air environment around a material can have a significant effect on the amount of oxygen diffusion that occurs within the material. For a crack that is open to the surface, a protective oxide layer forms on the fracture surface and instigates the oxygen diffusivity process. At some point, the oxide layer acts to passivate the material and prevent any additional environmental effects.

There are two different types of oxygen diffusion which occurs as a result of environmental exposure: short range diffusion and long range diffusion. Short range diffusion is defined by an oxide layer forming at the crack tip. The depth is controlled by the material parameters, geometry, and the applied load. Long range diffusion is defined by oxygen penetration on grain boundaries and slip planes. The presence of

oxygen atoms causes an embrittled effect on the grain boundaries and eliminates the crack growth barrier. The grains then act as a crack growth barrier and the subsequent crack growth proceeds along an intergranular path (Andrieu & Molins, 1992).

The rate of oxygen diffusion is governed by the inelastic strain energy density through an Arrhenius formulation shown in the equation below,

Equation 3 Arrhenius Equation

$$D_g = D * \exp\left(\frac{-Q_g'}{RT}\right) = D * \exp\left(\frac{-Q_g' - f(W_p)}{RT}\right)$$

where D is the diffusion constant, D_g is the diffusivity value of the grain boundary, Q_g' is the representative activation energy of grain boundaries, R is the gas constant, T is the temperature, and W_p is the inelastic strain energy density of the grain boundary. A high level of slip lines provides additional avenues for oxygen diffusion and a high loading frequency can help increase the density of slip lines present in a material. The amount of oxygen diffusivity into the grain boundaries remains constant, acting independent of the loading frequency. The resulting damage at the crack is a function of both cycle dependent crack growth and the contribution from the oxidation assisted crack growth (Vitek, 1978).

Zheng and Ghonem proposed a linear summation rule in 1992 as shown in the equation below. The equation is very similar to the superposition model proposed by Vanstone, however, the linear summation model is focused on the crack growth rate associated with environmental exposure time at temperature.

Equation 4 Linear Summation Rule

$$\left(\frac{da}{dN}\right)_{TOTAL} = \left(\frac{da}{dN}\right)_{CYCLE} + \left(\frac{da}{dN}\right)_{TIME}$$

Cycle dependent crack growth is essentially constant depending on material, applied load, and temperature. The time dependent portion of crack growth is more variable

as a function of environmental and dwell time effects on the rate of crack propagation (Zheng & Ghonem, Part II, 1991). The environmental effects exacerbate the time dependent crack growth mechanisms which operate at high temperatures to produce the total crack growth behavior.

Materials respond differently to oxygen diffusion based on static versus cyclic loading. Under static loading conditions, the oxidation products may cause crack tip blunting by making the material act in a more ductile fashion and cause crack retardation in an air environment. Under cyclic loading, the repeated cycles will increase the amount of oxygen adsorption onto the fracture surface. This reduces the surface energy and creates a better environment for voids which can help accelerate crack propagation (Shahinian & Sadanada, 1989). From a different perspective, Grandt claimed that diffusion products building up on the fracture surface can cause oxide induced closure. The accumulation of oxides can physically lock the fracture surface at a certain displacement and it may require an increase in load to have enough energy to overcome the barrier and continue propagating (Grandt, 2004).

2.1.2 Creep Crack Growth

Creep crack growth is a crack growth mechanism which is altered by temperature-activated creep mechanisms. Traditionally, creep is associated with a static load at high temperature, but this does not prevent the effect from occurring under cyclic loads. There are two stages of creep crack growth: initiation and growth. Material deformation occurs ahead of the crack tip per the creep strain law. Crack growth initiation under creep conditions is controlled by dislocation build up at the crack tip. The material will deform according to the creep strain law and does not depend as much on the plastic zone near the crack tip. Crack tip opening displacement has to reach a critical dimension in order for crack propagation to occur as a result of creep conditions (Vitek, 1977).

In 1978, Vitek proposed a theory of diffusion controlled intergranular creep crack growth in brittle materials. The theory is based on the concept of oxygen diffusion initiated by an oxygen environment at elevated temperatures. More specifically, the elevated temperatures activated cavity formation on the grain boundaries in the loading direction leaving open sites which were available to accept oxygen atoms and promote additional diffusion. Any cracks in the material will help focus the diffusion at the stress concentration area near the crack tip. Once the onset of creep occurs for the alloy, the oxygen atoms diffuse away from the crack tip towards the grain boundaries as a lowest energy configuration for diffusion. Pre-existing flaws in the component under these conditions will be subject to crack growth mechanisms, which the creep-induced diffusion may force the crack propagation into an intergranular progression. The build of diffused atoms along the grain boundaries can also cause stress relaxation in the area ahead of the crack tip. In this theory the crack propagation rate is limited by the upper limit on the rate of diffusion (Vitek, 1978).

Some of the principal drivers for creep crack initiation are void growth and coalescence at grain boundaries. There are several different void shapes that typically appear in materials, they are either round or spherical in shape. Prakash et al. showed that most creep fractures occur at triple points where three voids form a wedge shape. Grain boundary movement also influences the creep rate. Studies have shown that IN718 is sensitive to oxidation, especially along the grain boundaries, which are the lowest energy path for oxygen motion (Prakash, Walsh, Maclachan, & Kcrunsky, 2009).

Stress Accelerated Grain Boundary Oxidation (SAGBO) is the process by which the amount of loading on a material contributes to the speed of grain boundary oxidation. As previously discussed, this grain boundary oxidation causes an embrittled effect in the grain boundaries of a nickel based material and forcing the crack growth in the material into an intergranular progression. Since most of these reactions occur at elevated temperatures, there is typically also some creep

cavitation ahead of the crack trip which contributes to the overall increase in crack growth progression. Krupp et al. claims that oxygen-driven crack growth behavior does not require the formation of oxides, but rather that the elemental diffusion behavior within the grain boundary per the Hull-Rimmer Mechanism was a more important factor. The stress applied to the material acts as the driving force for diffusion with temperature acting as a catalyst (Krupp, Kane, Pfaendtner, Liu, Laird, & McMahon, 2004). The Hull-Rimmer Mechanism is a projection for diffusion based cavity growth where an intergranular cavity under loading expands from atomic diffusion from the cavity surface to the adjacent grain boundary (Krupp, Kane, Liu, Dueber, Laird, & McMahon, 2003). To summarize, higher loads can increase the amount of cavity growth in the grain boundaries, further weaken the grain boundaries, and encourage intergranular crack growth.

The creep crack growth rate is directly connected to the amount of dislocation motion which works to preferentially align the grain boundaries as a low energy crack growth path. The rate of creep progression drives the amount of dislocation motion in the applied load directions, while the remaining grain boundaries remain stationary. Crack growth can initiate from creep cracks under high temperature environmental conditions as a result of cavity formation and growth. As the temperature increases, the amount of oxidation increases which can increase the creep rate and the resulting creep crack growth rate. (Andersson, Persson, & Hansson, 2001). The crack growth rate and creep crack growth may not always be separate concepts and may both contribute to the overall crack growth rate in some situations.

2.1.3 Time Dependent Crack Growth Modeling

Both the superposition and linear summation rule are limited in the way that they are currently applied because the models assume that the time dependent effect is fully activated for the equations to be accurate. While they are both highly

accurate in a fully time-dependent crack growth regime, there is no consideration for partially converted or mixed mode material behavior included in this model. Current creep crack growth models are also limited by the temperature of the system. Once material operates above the dwell transition temperature, the models assume that the crack is controlled by the time dependent crack growth mechanism. This provides a signal to the modeler to include effects such as crack retardation and creep effects when creating a life assessment method. This research initiative and test program seeks to include more test parameters in the decision as to whether a component will operate under cycle dependent or time dependent crack growth mechanisms.

2.2 Fatigue Crack Propagation Mechanisms

2.2.1 Linear Elastic Fracture Mechanics

One of the easiest ways to discuss the transition between cycle dependent and time dependent crack growth is to summarize some of the concepts associated with cycle dependent crack growth. Linear Elastic Fracture Mechanics or LEFM is a standardized approach to fatigue crack propagation which depends on elastic behavior of material under an applied load. LEFM encompasses an overall system of fatigue crack growth prediction with an inclusive set of equations (Grandt, 2004). LEFM theory assumes that crack growth starts from a pre-existing crack and that cracks are mathematically sharp in order to propagate. The prediction system includes several key concepts which will be discussed below, but the overall main concept focuses on the stress intensity factor (K) as a representation of the outside load and its effect on a specific component (Boman, 1992). As the name suggests, the model predicts that the material will have a linear response under normal crack growth conditions.

Per Boman, there are three stages of crack growth. Stage 1 is the short crack growth regime where the crack size is on the order of microstructural levels. In Stage 2 crack growth the crack size is large compared to the microstructure and the growth rate is microstructure independent. Stage 3 crack growth is the static regime where the crack size is on the same order of magnitude of the smallest component features (Boman, 1992). According to Jahed et al., the definition of crack growth is broken down into two stages with different modes. During primary crack growth, the component undergoes Mode II crack growth where shear components are driving the crack growth behavior. Following primary crack growth, the component switches to Mode I crack growth where normal components drive the crack growth behavior pulling the two halves apart (Jahed & Varvani-Farahani, 2006). Generally, Stage 2 crack growth is predicted using the Paris model.

The Paris model was the original fatigue crack growth model which was used to predict behavior at slow fatigue crack growth rates (Newman, 1999). In practice, the Paris model is usually applied during Stage 2 crack growth where a linear relationship has been observed in a plot of the crack growth rate in comparison to the stress intensity factor. The stress intensity factor is an equation used to assess the applied load at the crack tip. The most generic version of the stress intensity factor (K) is

Equation 5 Stress Intensity Factor

$$K = \sigma\sqrt{\pi a}\beta$$

Where σ is the applied load, *a* is the crack length, and β is a geometry factor that can be altered for each specific situation. During testing, the applied load is typically increased as the number of cycles increase. This is known as an increasing ΔK test. To analyze the results, the ΔK value is typically plotted against the crack growth rate expressed as da/dN or the change in crack length over the number of cycles. For the Paris model, the data is a plotted as da/dn versus ΔK and a trendline is fitted through the data using a Power Law expression. The resulting equation is known as the Paris Law.

Equation 6 Paris Law

$$\frac{da}{dN} = C\Delta K^m$$

In the Paris Law, C and m are material constants which assist with the curve fit (Grandt, 2004). While the Paris Law is used frequently to express the relationship between the crack growth rate and the applied load in cycle –dependent crack growth, the expression is not as meaningful under time-dependent crack growth because it does not account for time. For this project, a different type of Power Law fit will be applied to account for the time-dependent considerations.

2.2.1.1 Brittle Fracture

The Griffith Theory is a fracture criteria equation based on the energy balance in brittle materials. As a crack propagates, the theory requires that the loss of strain energy must be equal to the increase in surface energy. For brittle materials there is a competition between dislocation emission and interatomic bonds breaking to cause cleavage. One of the difficulties in predicting the crack growth propagation of brittle materials is predicting the amount of shielding from dislocations. After dislocations are emitted and contribute to the changes to the crack tip, they can also build up and act as a barrier to subsequent crack propagation (Beltz, Lipkin, & Fischer, 1977).

The geometry of the material can alter fatigue crack growth behavior to promote or inhibit propagation. One of the ways that geometry is accounted for is through stress concentration factors (Hoshide & Socie, 1987). There are a variety of stress concentration factors that can be used in equations; however, one of the most commonly used values for crack growth is a K_t value. The stress concentration factor is a ratio of the nominal or minimum applied load in comparison to the maximum applied load which helps account for the geometry that can act to localize the material stress response. The generic equation for the stress concentration factor is shown in Equation 7 (Grandt, 2004).

Equation 7 Stress concentration factor

$$K_t = \frac{local\_stress}{remote\_stress} = \frac{\sigma_{local}}{\sigma_{remote}}$$

The equation is frequently applied to notch or circular geometries. At higher K_t values, the geometry has a greater influence on the load distribution and the subsequent crack growth behavior (Budynas & Nisbett, 2011).

The effect of the stress concentration factor can be determined by assessing the geometry of the notch or hole feature using the Peterson equations. Peterson developed a series of equations to calculate the stress gradient from a geometrical feature and determine how far the stress concentration extends into the bulk material before the effect is negligible. For this research program, two different notch geometries were evaluated and tested, K_t = 1.5 and K_t = 3.0. The generic Peterson equation for a notch is

Equation 8 Peterson Notch Equation

$$K_t = \frac{2\left(\frac{d}{r}+1\right)\sqrt{\frac{d}{r}}}{\left(\frac{d}{r}+1\right)\arctan\sqrt{\frac{d}{r}}+\sqrt{\frac{d}{r}}}$$

Where d is the notch depth and r is the notch radius. The stress gradient is measured as the stress versus the ratio of the notch radius over the notch depth (r/d). A shallow notch is limited by the fatigue capability of the material while a sharp notch is limited by the fatigue crack growth capability (Noda & Takase, 1999).

Crack growth in brittle materials is characterized by crack branching caused by particles or grain interfaces in the material which forced the crack tip to change direction. The microstructure of naturally brittle materials, such as ceramics, has a large effect on the crack growth rate in ceramics. (Ritchie, 1999).Time dependent crack growth does not follow the predictions embedded in the LEFM system. There are some physical responses which align with the underlying principles of LEFM, but it cannot be called a true LEFM response.

2.2.1.2 Ductile Fracture

Ductile fracture occurs when plasticity levels overrule the influence from the Griffith theory. This process creates a plastic zone around the crack tip. The dislocations in ductile fracture are emitted from the crack tip which helps to create the plastic zone. The crack propagates through the material as more and more dislocations are emitted (Zheng, Rosenberger, & Ghonem, 1993). The fracture surface of a ductile fracture is characterized by striations or ridges on the crack face. The rate of crack propagation directly correlates to dislocation emission which forms the ridge on the surface of the fracture face. Each striation can be connected to a loading cycle and can be used to measure the number of cycles that a material experiences during testing or operation (Ritchie, 1999); (Boman, 1992).

When a directional load is applied to a material, slip will occur along the preferred planes and the initial dislocation will formed along those same planes. The material crystal structure determines the preferred slip plane and the resulting dislocation density. Following the initial dislocation effect, an increasing number of dislocations form as a result of the Frank-Read process. The plastic deformation around the crack tip creates the optimal environment for dislocation multiplication (Frank & Read, 1950). The stress concentration around the crack tip creates a plastic zone which is sometimes referred to as a "K-dominated zone." The radius and shape of the plastic zone are typically determined by the stress state. As the plastic zone size gets too big, the stress concentration becomes a less important factor (Schjive, 2001).

To summarize, time dependent crack growth does not strictly follow the crack growth rate trends of LEFM, but it does display characteristics of both ductile and brittle fracture, especially in the transition regions. Under low temperature or low stress conditions, the mixed mode region may contain both intergranular and transgranular features.

2.2.2 Elastic-Plastic Fracture Mechanics

Elastic-plastic fracture mechanics is a modification on the standard to crack growth modeling that allows for a greater influence of plastic deformation in contrast to some of the concepts in LEFM. While LEFM has been shown to be a highly accurate approach for monotonic loading scenarios, an elastic-plastic approach may be more appropriate for cyclic loading crack growth scenarios. Elastic-plastic fracture mechanics also encompasses the concepts of continuum mechanics which have been used to model fatigue crack growth behavior.

Continuum concepts can also be used to evaluate the ductile versus brittle fatigue crack propagation response. There are some materials which behave as a purely brittle material or as a purely ductile material based on their crystal structure and atomic bonding. Typically the theory of continuum mechanics assumes that the crack is atomically sharp and then analyzes how the crack tip changes with applied load. Ductile materials emit dislocations prior to reach load levels to cause crack propagation, while brittle materials do not emit dislocations until after the load levels are above the needed amount to cause crack propagation (Beltz, Lipkin, & Fischer, 1977). There are other materials, however, which can transition between brittle and ductile behavior based on their energy release rate. Some models have shown that there is a brittle to ductile transition temperature. Cleri et al. performed an analysis looking at a molecular dynamics simulation using the Lennard Jones interatomic potential. The simulation assessed the energy barriers that had to be overcome in order to support dislocation motion. The dislocations near the crack tip were connected to stress relaxation and a crack tip shielding effect that actually increased the amount of energy required to maintain crack propagation. The effect is referred to as “crack tip blunting” (Cleri, Yip, Wolf, & Phillpot, 1997).

Crack tip blunting also frequently occurs in time dependent fatigue crack growth and can act to limit the crack propagation. This is another example of where the time dependent mechanisms do not completely align with the elastic-plastic model, but there are distinct features which are present in both.

2.2.2.1 Crack Tip Opening Displacement

Crack tip opening displacement or CTOD is a measurement of the distance that a crack is open and exposed. There are a variety of ways to measure CTOD and maintaining a consistent approach is vital to preserving the data quality in an assessment. The CTOD can be used to quantify both the driving force for crack growth as well as the amount of closure, when applicable. CTOD is typically measured by drawing two parallel lines behind the crack tip and measuring the distance between the lines. An illustration of CTOD measurements relative to the crack tip is shown in the figure below.

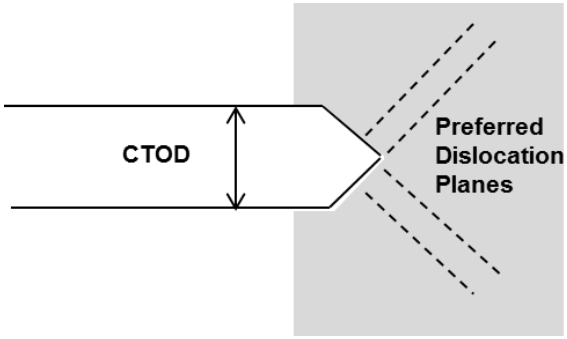

Figure 2.3 An illustration of the Crack Tip Opening Displacement measurement relative to the crack tip

There are two methods to calculate crack-opening stresses. One method is to assess the contact-K analyses on crack opening displacement, while the other is to look at the crack tip opening displacement for constant K_{max} testing near the threshold (Newman, 1999).

Per Boman, CTOD is characterized by the growth of the plastic zone with increasing load cycles in the wake of the crack tip. The zone acts as a long, thin band of plastic deformation that follows the surface of the crack faces. This initial, smaller zone is called the compressive zone. As the number of cycles increases, the zone size increases and the CTOD also increases. Once the width of the zone increases and it is more comparable to the length of the zone, the driving force will be eliminated and the zone will stabilize. This larger, more stable version of the zone is called the expansive zone. In terms of crack propagation, the compressive zone promotes crack growth, while the expansive zone can cause crack retardation (Boman, 1992). This is more frequently referred to as the Dugdale Strip Model (Dugdale, 1960).

2.2.3 Factors Which Can Affect Fatigue Crack Growth

There are several test parameters which can affect fatigue crack growth behavior. Tests are often designed to simulate the service condition of a component operating in an engine. This can include concepts such as the test frequency, waveform, and applied stress ratio or R-ratio.

The frequency of the applied load can also have a strong influence on the fatigue crack growth rate at elevated temperature. Weerasooriya looked at crack length in Inconel 718 as both a function of low frequency and high frequency loading. The frequency response was divided into three categories: cycle dependent, mixed mode, and time dependent. The crack growth rate increases with decreasing frequency, therefore low frequency testing was categorized as time dependent or frequency dependent behavior. Mixed mode crack growth behavior was affected by environmental conditions in addition to the frequency condition. Cycle dependent or frequency independent crack growth has a constant crack growth rate and usually occurs at higher frequencies for an elevated temperature condition. At higher frequencies, the crack growth process is occurring too fast for environmental effects to affect the material (Weerasooriya, 1987).

The way that load is applied to the specimen is called the waveform in a testing application or mission cycle in a component based application. Most fatigue crack growth testing has a truncated type of waveform to simulate a real life loading condition such an in-flight mission profile in aerospace applications. Within a waveform, the ratio of the minimum stress to the maximum stress is called the R-ratio,

Equation 9 R-ratio

$$R = \frac{\min stress}{\max stress} = \frac{\sigma_{\min}}{\sigma_{\max}}$$

The R-ratio indicates whether the loading is applied purely in tension or whether the load is also applied in compression. For example, the load can be applied from zero to a positive maximum level in tension or from a negative minimum value to zero in compression.

There are four common types of waveforms: balanced triangular, trapezoidal, trapezoidal with dwell, and sinusoidal. A balanced triangular waveform has a minimum and maximum load level, the applied load cycles between the two points with an equal amount of time to ramp up and ramp down. A trapezoidal waveform has four segments that get continually repeated: (1) ramp up, (2) hold at maximum load, (3) ramp down, (4) hold at minimum level. This type of waveform is thought to be consistent with an aerospace application where the ramp up is take-off, the hold at maximum load is indicative of cruise time, the ramp down is representative of landing, and the hold at minimum load is the rest period between flights. A trapezoidal waveform with dwell is the same cycle with a longer hold time at the maximum load point. This dwell period can vary between multiple seconds and over an hour to best simulate the cycle of interest for testing purposes. The type of waveform is more influential when the test frequency is slower; at higher frequency the rate of loading overpowers the influence of the type of loading (Tong, Dalby, Byrne, Henderson, & Hardy, 2001). A sinusoidal waveform fluctuates between minimum and maximum loading following a sinusoidal function curve. An illustration of the different types of waveform loading is shown in Figure 2.4.

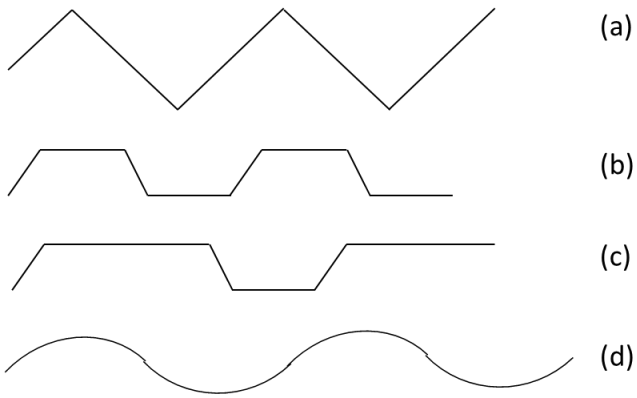

Figure 2.4 Four common types of fatigue crack growth waveforms: (a) Balanced Triangular, (b) Trapezoidal, (c) Trapezoidal with dwell, and (d) Sinusoidal

There is some disagreement over whether or not dwell conditions would exist with a high degree of probability (Wanhill, 1999). However, as industry seeks to increase the efficiency of aerospace engines and use less fuel, the operating temperature of the disk material is continuously increasing making it more and more likely for a dwell period to exist.

The Foreman Equation helps quantify the amount of overload required for crack retardation to occur. The crack growth rate with overload is calculated using the equation below.

Equation 10 Foreman Equation

$$\frac{da}{dN} = \frac{C_f \Delta K^{n_f}}{(1 - R_{eff})K_c - \Delta K}$$

C_f = Foreman coefficient n_f = Foreman exponent
K_c = fracture toughness R_{eff} = effective load ratio

With increasing temperature, the yield stress of the material decreases and the plastic zone size increases (Barker, Johnson, Adair, Antolovich, & Staroselsky, 2013). This research program is testing a variety of load sequences and will correlate the results to the crack growth models. The Foreman equation is one possible method that could be used to correlate the overload crack growth data in the associated modeling work.

2.2.4 Physical Indications of Fatigue Crack Growth Behavior

The physical appearance of the fracture surface can provide strong indications about the crack growth mechanisms. Fatigue crack growth behavior can be documented using a Scanning Electron Microscope (SEM) to produce a high magnification image of the surface topography. Broek published a summary of fracture surface morphology findings. The research defined several types of fracture surfaces. Intergranular growth is a fracture surface that moves along grain boundaries and is usually attributed to a brittle response or embrittlement in a ductile material. Transgranular growth is a fracture surface that moves through the grains in a material. In cyclic loading, transgranular fracture surfaces have ridges or striations that represent changes in loading. The research also described the practice of apply tilt during the SEM evaluation to enhance the surface features and the visibility of striations (Broek).

VanStone also proposed a term to describe physical fracture surface behavior, “crack tunneling,” where the crack length through the specimen cross section is compared to the crack length measured along the surface of the specimen. This creates a pinched appearance to the fracture surface. An illustration of a fracture surface with crack tunneling is shown in Figure 2.5.

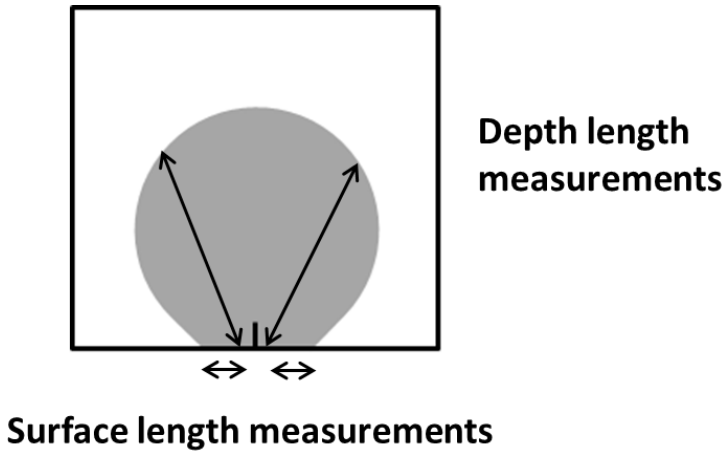

Figure 2.5 Schematic of crack tunneling measurements on the face of a fracture surface

The two measurements are averaged to get the final crack tunneling measurement.

Equation 11 Crack Tunneling Equation

$$Tunneling = length_{avg,surface} - length_{avg,depth} = \left|\Delta length\right|$$

The amount of tunneling decreases with overload points (VanStone, Gooden, & Krueger, 1988). Crack tunneling occurs when the crack length going into the specimen is longer than the surface crack length. The amount of tunneling has been shown in increase with increasing temperature, increasing overload values, and increasing dwell times (VanStone, Gooden, & Krueger, 1988).

2.3 Retardation & Crack Closure Models

Crack retardation occurs when a crack reaches a single max load that is greater than the rest of the maximum loads causing the crack growth rate to slow down. The overload causes an increase in the size of the plastic zone depending on the level of loading. After overload, the material elastically unloads leaving a compressive local stress. The amount of retardation increases with rapid crack growth rates (VanStone, Gooden, & Krueger, 1988). Plasticity induced closure causes retardation after an overload cycle. The overload causes plastically elongated material in the crack wake. This creates a large plastic zone at the crack tip and promotes blunting (Schjive, 2001). An overload can also cause residual stresses to form ahead of the crack tip which can reduce the effect of the stress intensity factor and helps to retard the growth rate (Grandt, 2004).

As mentioned in Section 2.2.2.1, the Dugdale Strip Model for crack growth focuses on the plastic zone growth under loading. Riedel presented a separate theory on how the Dugdale Model could be applied to time dependent crack growth under creep conditions. As stated above, creep activated crack growth mechanisms cause stress relaxation near the crack tip. Riedel's theory proposed that there is a connection between the stress intensity factor and the crack growth rate assuming that both small scale yielding and a steady state crack growth condition exists. Crack

propagation occurs when a critical amount of strain has accumulated at the crack tip or the CTOD. There are some limitations to applying the Dugdale model, including the fact that the model did not include the size of the plastic creep zone (Riedel, 1977).

The surface condition of the material can affect the fatigue crack propagation properties of a material. The surface roughness can affect the amount of closure that a material experiences. Crack closure associated with surface roughness is called asperity induced closure. Shot peening can also alter the crack propagation rate. The shot peening process creates a compressive residual stress on the surface of the material which can relieve the stress build up at a pre-existing surface flaw and prevent it from propagating (Grandt, 2004), (Schjive, 2001).

Evans also looked at the overall combination of environmental and creep effects on the crack closure occurring in the material. The goal was to improve the predictive capability and assist in predicting crack growth under a dwell regime. Facet formation on fracture surfaces is ultimately connected to slip plane movement in the material with an applied load. Evans found that as temperature increased, the material mechanisms switched from being load dependent to being creep dependent (Evans, 2004).

Plasticity induced crack closure leads to crack tip blunting (Andersson, Persson, & Hansson, 2001). Plastic deformation occurs at the crack tip and changes the shape of the plastic zone around the crack tip. Closure or blunting occurs during the unloading cycle. The presence of plasticity induced closure can be confirmed via the CTOD measurements (Schjive, 2001).

CHAPTER 3. APPLICATION OF THEORETICAL MODELS

This analysis seeks to focus on nickel based superalloys because of their applicability to hot section critical rotating components in an aerospace application. Nickel based superalloys have high strength levels associated with the precipitates embedded in the matrix. Some of those precipitates are γ' particles which can act as a barrier to dislocation motion or alter the preferred slip direction (Prakash, Walsh, Maclachan, & Kcrunsky, 2009). Crack propagation occurs primarily in the preferred crystallographic direction with the applied loading. After the crack tip opening displacement levels have adjusted, the crack propagation shifts to grow perpendicular to the max opening stress (Reed & King, 1992).

Previous time dependent crack growth models, such as the VanStone superposition model and the linear summation model from Zheng et al., focused solely on the temperature exposure as an "on/off switch" to include time dependent constraints into the model (VanStone, Gooden, & Krueger, 1988) (Zheng & Ghonem, Part I, 1991). This research program seeks to include additional parameters into the model such as geometry, dwell time, applied load, and type of mission or waveform. The theory behind this program was that the competing mechanisms in time dependent crack growth are enhanced or retarded by these factors. For example, at high temperature and low load levels, the effect of time dependent crack growth may be minimized in comparison to material at both high temperature and high load levels. These correlations are combined to create a mechanism map of cycle-dependent parameters, time-dependent parameters, and mixed mode parameters.

Previous authors have discussed creep crack growth and environmentally affected crack growth as two different topics. This research program assumes that there is no need to keep these two concepts separate in the predictive modeling.

Creep crack growth is activated by high temperature environment with an applied load. Environmentally assisted crack growth is also activated by a high temperature environment under an applied load. While creep crack growth testing is typically performed under a static load and environmentally assisted crack growth is assessed on both static and cyclic loading, a cyclic load does not prevent creep activated effects from occurring in the material. Therefore, this research will look at both creep effects and environmental degradation effects in the test program as a part of time dependent crack growth.

Based on the material composition and the grain size, a couple predictions were made as to the material response to the microstructural pre-disposition to transition. The IN-718 is more unpredictable than the other alloys based on some of the competing mechanisms which affect transition. IN-718 material is the mostly likely to experience creep effects based on a lower level of solid-solution strengthening from γ’ particles and carbides. At the onset of creep effects, a material can experience stress relaxation in the crack tip plastic zone and start to see some closure which can work to prevent transition. IN-718 is also known to respond more quickly to oxygen diffusion and experience embrittlement which will activate a transition from cycle-dependent to time-dependent crack growth. Waspaloy has a higher creep capability and a lower strength indicating that it will see less closure effects and more bulk strain response making it more likely to transition. Udimet-720 has the highest creep capability and the highest strength levels making it even more likely to transition than the other two alloys assuming that the same conditions were applied across all three alloys to normalize the response.

CHAPTER 4. EXPERIMENTAL METHODS

4.1 Mechanism Map

The mechanism map was constructed for each dwell period with a variety of test parameters to target transitional periods. The temperature range is set for values both above and below the dwell transition temperature. The load range is set from a relatively low value up to a relatively high value. For a set dwell period (e.g. 5 minutes, 15 minutes, 60 minutes), it is assumed that low temperature and low load combinations will maintain cycle dependent crack growth characteristics. At high temperature and high load values, the material is expected to consistently transition to time dependent crack growth characteristics. At the intermediate values, there may be a mixed mode transition period where there are characteristics of both cycle dependent and time dependent crack growth.

The results of the mechanism mapping were used to assist in choosing test conditions such as temperature, geometry, load level, and dwell period while predicting whether the component would display evidence of a cycle dependent, time dependent, or mixed mode response. The goal of the program is to correlate the results of the models against the physical specimens. The fractography and crack propagation rate of the test specimens should indicate the level of confidence in the model.

4.2 Material

Three different nickel-based superalloys were tested in this study to assess the fatigue crack growth behavior: Udimet 720, Inconel 718, and Waspaloy. Fatigue crack growth specimens were removed from the both the rim and web region of turbine disk forging material. These two regions were selected to represent the

parts of the disk that are most likely to experience cracking in service. Nickel based superalloys are all strengthened by γ’ or γ’’ precipitates, but the different compositions can have an effect on the performance capability of the material (Krupp, Wagenhuber, Jacobs, & McMahon, 2005).

The Udimet 720 (U-720) material for testing was removed from turbine wheel forging that was procured under a Rolls-Royce proprietary specification. The material was solution and precipitation heat treated. The average grain size of the material was ASTM 10 – 11.5. Based on previous research, the dwell transition temperature of U-720 was approximately 500°C.

The Inconel 718 (IN-718) material for testing was removed from a fan disk forging that was procured under a proprietary specification similar to AMS 5663. The material was solution and precipitation heat treated. The average grain size of the material was ASTM 10.5. Based on previous research, the dwell transition temperature of IN-718 was approximately 475°C (AMS 5663, 2009).

The Waspaloy material for testing was removed from a turbine wheel forging that was procured under a proprietary specification similar to AMS 5704. The material was solution and precipitation heat treated. The average grain size of the material was ASTM 9. Based on previous research, the dwell transition temperature of Waspaloy was also approximately 500°C (AMS 5704, 2009).

Three different test geometries were used in this program. An example illustration of the specimen layout within the forging is shown in Figure 4.1. This illustration shows the layout applied to the Waspaloy forging. All specimens were removed in a chordal orientation. The effect of other specimen orientations on the fatigue crack growth rate is out of scope for this research program.

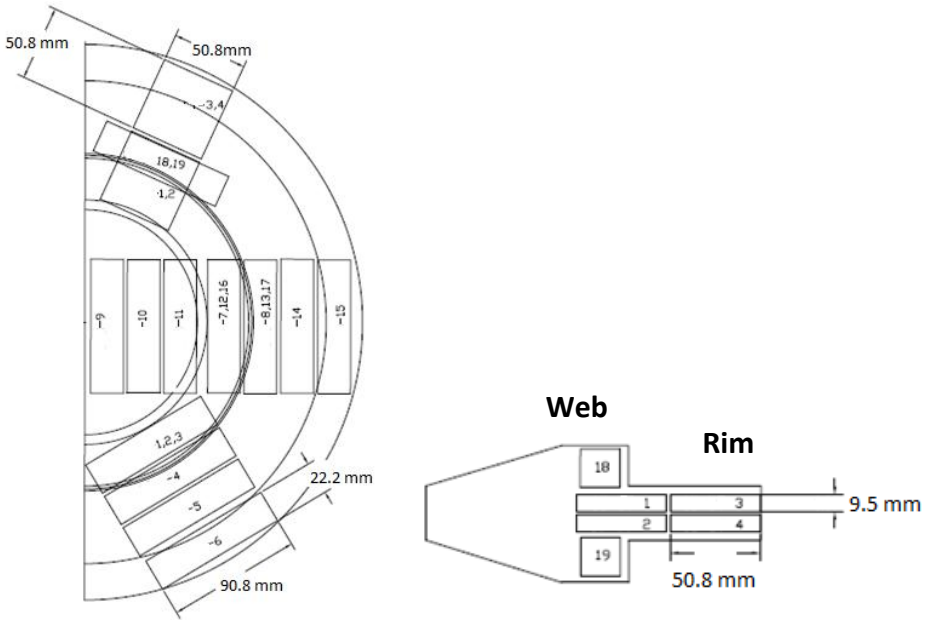

Figure 4.1 An example schematic of the crack growth specimen layout within the forging material

There are three types of specimens which are used in the test program. The first type of specimen was a compact tension specimen with a radial crack located on the outer diameter location of the specimen. The compact tension specimen was designed to be in compliance with ASTM E647-00 (ASTME647-00, 2001). The second type of specimen was a corner crack specimen with a square gage cross section. The third type of specimen was a surface flaw or Kb bar specimen which has the same general geometry as a corner crack specimen with a notch in the center of the gage section. A graphical representation of the corner crack specimen and compact tension are shown in Figure 4.2.

(a) 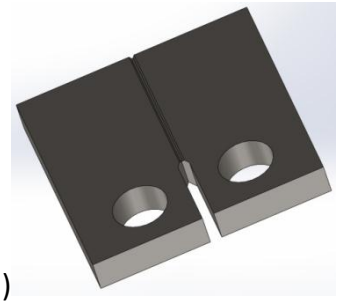 (b) 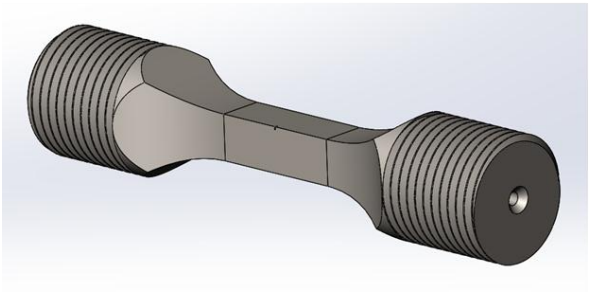

Figure 4.2 Visual representation of (a) corner crack specimen and (b) compact tension specimen

The notch geometry in the Kb bar was altered to have a low K_t specimen with a stress concentration factor of 1.5 and a high K_t specimen with a stress concentration of 3. Both configurations have rounded, shallow notch geometries. Both the corner crack and Kb bar specimen have round threaded ends which are sized for the test frame interface.

4.3 Test Methods

All fatigue crack growth specimens were tested on a servo-hydraulic test frame. This facilitates a cyclically applied loading and unloading process. The creep crack growth specimens were tested on a creep frame with a static load. The crack growth specimens were tested using a trapezoidal waveform with a dwell applied at the maximum load when applicable. For a test profile with no dwell period, a one second time period was applied to each segment (1-1-1-1). For those dwell specimens, the max load time was varied between 5 minute, 15 minute, and 60 minute dwell time (1-dwell-1-1). An example of the load profile is shown in the figure below.

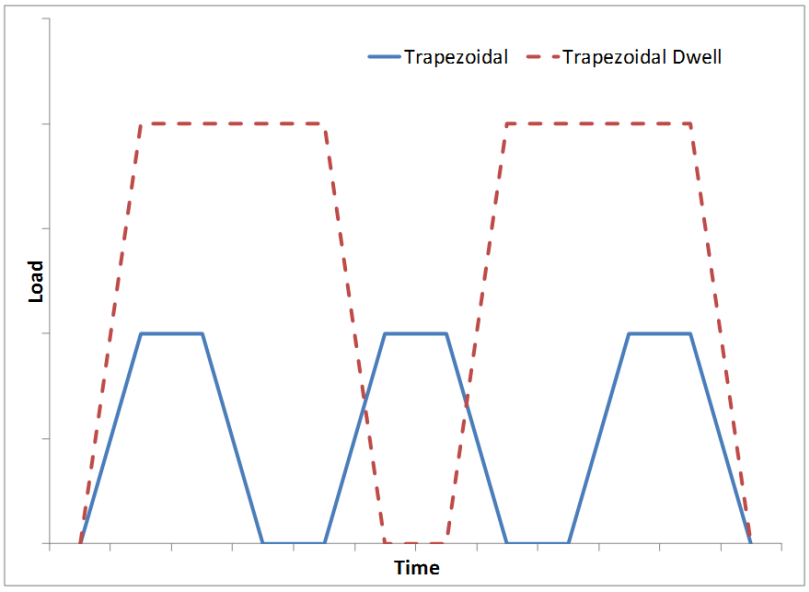

Figure 4.3 A Plot of a trapezoidal waveform compared to a trapezoidal waveform with dwell periods at the maximum load

Crack monitoring was performed using a Direct Current Potential Drop (DCPD) technique. The DCPD operates by tack welding a small set of wires on either side of the pre-crack connected to a voltmeter and a DC power source. The system also includes a recording device which documents the changes in voltage over the duration of the test. During testing an electrical current is applied to the system and the measurement of the electrical current changes as the CTOD distance increases. This change in electrical current is used to calculate the crack growth as a function of cycles. The change in crack size will affect the amount of current that is monitored in the voltmeter and provide a summary of the crack progression (ASTME647-00, 2001).

All specimens were pre-cracked at room temperature prior to testing at an elevated temperature. In order to create crack initiation, a small notch is made in the center of the gage section using Wire Electro-Discharge Machining (EDM) and a small ΔK load is applied to cause the initiation site to grow into a short crack with a natural crack tip. Following the creation of a short crack, the temperature is increased and the starting ΔK load is applied to start the stage II crack growth. The wire EDM notch is applied at the corner of the corner crack specimens, while it is applied mid-way across the cross section for the Kb bar specimen on one surface.

In addition to DCPD monitoring, the crack growth test is periodically stopped in order to perform a heat tint operation in order to validate the DCPD values. The heat tint time and temperature is sensitive to the type of alloy. The heat applied to the specimen adds color to the surface of the specimen as a result of the oxidation. After each quantized amount of crack growth the heat tint changes color slightly providing the appearance of rings of growth emanating from the pre-crack origin. For this test program, the heat tint was applied to all three alloys at 650 °C for 30 minutes to an hour depending on the time required to see a color change.

4.4 Test Matrix

The test matrix for the research program was designed to test out several different theories related to the concept of time dependent fatigue crack growth. The testing was structured in order to isolate some of the conditions and test combinations of other conditions. There are six major sub-categories of testing that are broken out below with a description of the test goal and a summary of the specimens tested. The six major categories of testing are creep crack growth, time dependent crack growth, geometry, temperature, load sequence, and material. The larger research program contained several different sets of test specimens with repeated specimens at specific conditions to introduce the concept of repeatability. This summary will focus on a selected number of specimens in order to illustrate a quantitative comparison of crack growth rates and the way that transition mechanisms contribute to the rate. A complete outline of the test conditions included in the larger research program is included in Appendix A.

In terms of test parameters, there are several conditions that were applied to all specimens. All testing was performed at an R-ratio of 0.05, or the R-ratio closest to zero that can be performed in crack growth without causing the fracture surfaces to interact during the test cycle. The specimens were initially notched via wire EDM and then pre-cracked or cycled at room temperature in order to produce a natural crack tip to simulate the type of initiation that occurs in a component. In order to take full advantage of the cross section of the specimen, the notch and pre-crack were produced to be as small as possible.

4.4.1 Baseline

A series of tests were performed on material removed from the same forgings in the same geometry as the subsequent tests in order to establish baseline test results. These results will be used as a comparison point for the testing with dwell and overload conditions. The baseline testing was performed under cycle

dependent conditions. There was no applied dwell time and the temperatures were varied across the same temperature range as the rest of the research program. Baseline crack growth testing was performed per ASTM E647-00 on a servo-hydraulic test frame with an increasing ΔK load (ASTME647-00, 2001).

4.4.2 Creep Crack Growth

Creep crack growth is performed by applying a static load to a notched specimen in the creep temperature range to evaluate the crack growth rate under the influence of creep. The testing is typically performed on a Compact Tension (CT) specimen. The load can be applied to the specimen on either a static test frame or a servo-hydraulic test frame held in a static condition (ASTME1457, 2013). Alternatively, creep-fatigue crack growth is performed by applying a cyclic load under a similar temperature range. Depending on the temperature and waveform, this can be a cycle dependent or time dependent type of test (ASTME2760, 2010).

Most materials respond under a creep-ductile or creep-brittle response. In a creep-ductile response, the strain from creep and time dependent crack growth dominates the material behavior. In a creep-brittle response, crack growth occurs as a response to low creep ductility. Under creep crack growth there are two regions of behavior: (1) initiation period where creep damage starts to permeate the material, and (2) the steady state period where the crack grows over time (ASTME1457, 2013).

4.4.3 Temperature

Three temperatures were tested for each material to try and capture a temperature range above and below the predicted dwell transition temperature. An intermediate temperature was tested for each material to help interpolate between the outer bounds of the temperature range. The increments between temperatures in this test program were smaller than most other research programs to try and detect subtle changes in the crack growth behavior. One of the major goals of this

research initiative is to pinpoint the transition point where crack growth switches from time dependent “standard” crack growth to mixed mode cycle dependent crack growth. Three different temperatures were tested for each alloy. The temperature range tested for Waspaloy and U-720 was 540°C to 650°C. The temperature range tested for IN-718 was 470°C to 590°C based on the alloy temperature capability. The temperature tolerance of the test equipment is approximately 15°C from the nominal. The creep crack growth results for each alloy will be compared to the time dependent crack growth rates to determine the similarities between a static and cyclic load.

4.4.4 Geometry

One of the major parameters that are being evaluated by this research program is the effect of geometry on the crack growth rate under dwell conditions. The notch geometry of the Kb bar was altered in order to capture geometry effects. A high K_t and low K_t geometry were both included in the test matrix for comparison. Tests were performed on IN-718 material at three different temperatures on all three specimen geometries. The dwell time was held constant to isolate the temperature and geometry factors in these tests. The geometry specimens will be compared back to a standard corner crack configuration in the baseline testing to see how it affects the crack growth rate.

4.4.5 Load Sequence

The order in which load is applied can significantly affect the crack growth behavior of a material. One way that this was analyzed in this research program was through a discontinuous dwell cycle. Dwell cycle was applied per standard time dependent testing, but after a set period of time the dwell cycle was removed and a triangular waveform was applied for a set period of time.

The assumption is that crack tip blunting will occur under the dwell test period and then the triangular test period will re-sharpen the crack tip. Then the dwell waveform was reapplied for the rest of the test period.

Overload cycles are applied during testing to simulate a peak load followed by a smaller load applied in service or a mission profile. Typically overload loading makes the material more susceptible to plasticity induced closure and crack tip blunting (Schjive). For overload testing, standard crack growth testing was performed per ASTM E647-00 with a specific overload cycle added at the beginning of the load profile followed by the standard dwell period. The level of the overload loading value varied from 105% to 120% of the maximum load applied for the rest of the test profile. A visual representation of the overload mission profile is shown in Figure 4.4.

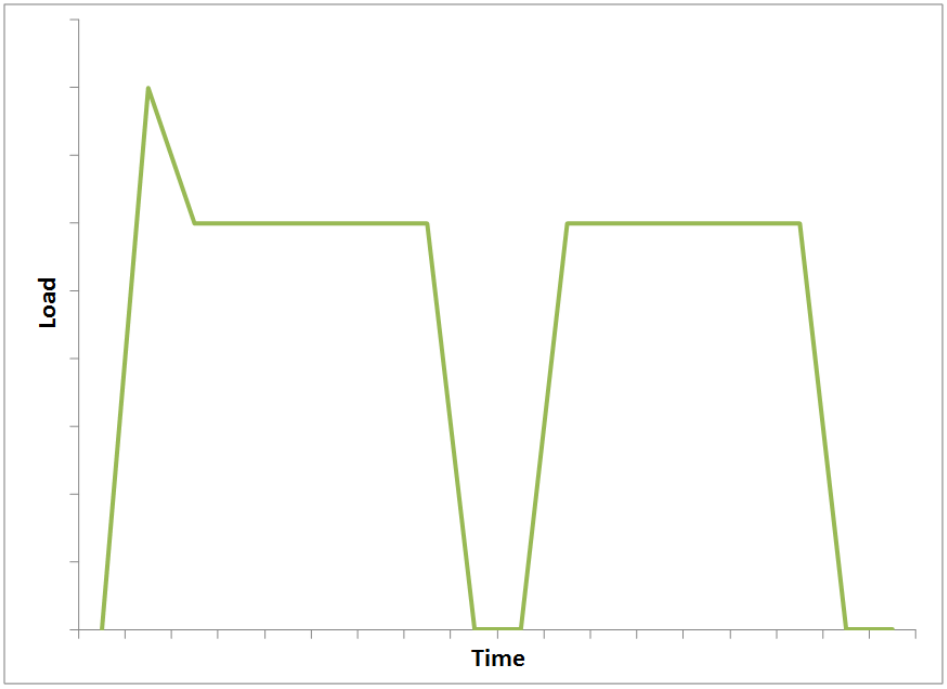

Figure 4.4 Plot of an overload mission profile on a trapezoidal dwell waveform

Overload testing was performed IN-718 material at two temperatures. The overload test results will be compared to dwell crack growth testing at the same temperature to determine whether retardation effects are visible in the crack propagation rate results.

4.4.6 Material

Several of the test conditions were consistent across all three alloys to help compare the results across the variants of nickel base superalloys. The microstructure of the test material was evaluated to document the condition of supply at different locations in the forging. The differences in the crack growth rate and fracture surface appearance will be discussed to bring context towards the grain size and the composition of IN-718, U-720, and Waspaloy material.

4.5 Laboratory Evaluation Technique

All fracture specimens were evaluated on a Scanning Electron Microscope. The fracture surfaces were inspected in a JEOL JSM-5900LV SEM instrument. The fracture surface morphology was assessed starting with the pre-crack region and spanning across the fracture surface until the overload region. As described in Section 2, transgranular crack growth progression is attributed to cycle dependent crack growth, while intergranular crack growth progression is attributed to time dependent crack growth. The Secondary Electron Imaging (SEI) beam was used to identify whether a crack progressed in a transgranular or intergranular fashion. Some specimens also exhibited secondary cracking branching off from the primary crack.

A macroscopic evaluation was also performed on the fracture surface to measure the amount of crack tunneling present under each condition. The colored rings from the heat tint operation provides a visual illustration of the crack growth

distance on the surface of the specimen in comparison to the crack distance through the center of the specimen cross section. Magnified images of the fracture surface were produced using a Keyence DHX digital microscope system. The scaled images were then used to measure the crack growth distance on the surface in comparison to the mid-section in order to determine the level of crack tunneling associated with each test condition. The microstructural analysis was performed on an Olympus microscope system. Two samples were removed from each forging at the rim and web locations to document the differences in grain size associated with the forging process.

4.6 Data Analysis

The crack growth data for the various tests must be processed in a way to assist with the comparison across all three types of testing and specimen geometries. Therefore, all of the crack growth data was plotted as the change in crack length over the change in time (da/dt) versus the test time (t). The data was plotted on a log-log scale and then normalized so that all of the properties would start at roughly the same initial crack rate and test time. This allows for a comparison of the crack growth rates. A power fit equation was applied to each data set to show the trend without the scatter in the data. While a Paris Law fit cannot be applied to all test types, the same fit can be applied to the rate data. The plots shown in the results section will compare the trend lines at each of the conditions.

CHAPTER 5. RESULTS

The results are a combination of the crack propagation data and the corresponding SEM fracture surface images. The crack propagation comparisons are targeted to assess the trend associated with a smaller number of parameters. The associated fracture surfaces will be used to analyze whether a set of test conditions operated under cycle dependent, time dependent, or mixed mode response. The macroscopic analysis will be discussed at the end of the results section in order to develop a hypothesis regarding the implications of crack tunneling. An arrow will be used on all fracture surface images to indicate the crack propagation direction.

5.1 Dwell Crack Growth Times

The first comparison made is between the creep crack growth and various dwell time results. One of the premises in this thesis is that there is limited difference between dwell crack growth and creep crack growth. Therefore the dwell crack growth and creep crack growth specimens were compared on the same plot for tests performed at the same temperature. The expectation is that the crack growth rate should be very similar across the two different types of testing. The crack growth rate data is plotted as the ratio for change in crack growth length over time versus the test time. Both the ratio data and the time data are normalized to present all data starting at the same location and assist in the slope comparison between test results and assist in the comparison between dwell crack growth testing and creep crack growth testing.

The IN-718 material was tested at a baseline with no dwell, with a 15 minute dwell, and under creep crack growth conditions. A plot of the creep crack growth and dwell crack growth results for IN-718 at 540°C is shown in Figure 5.1.

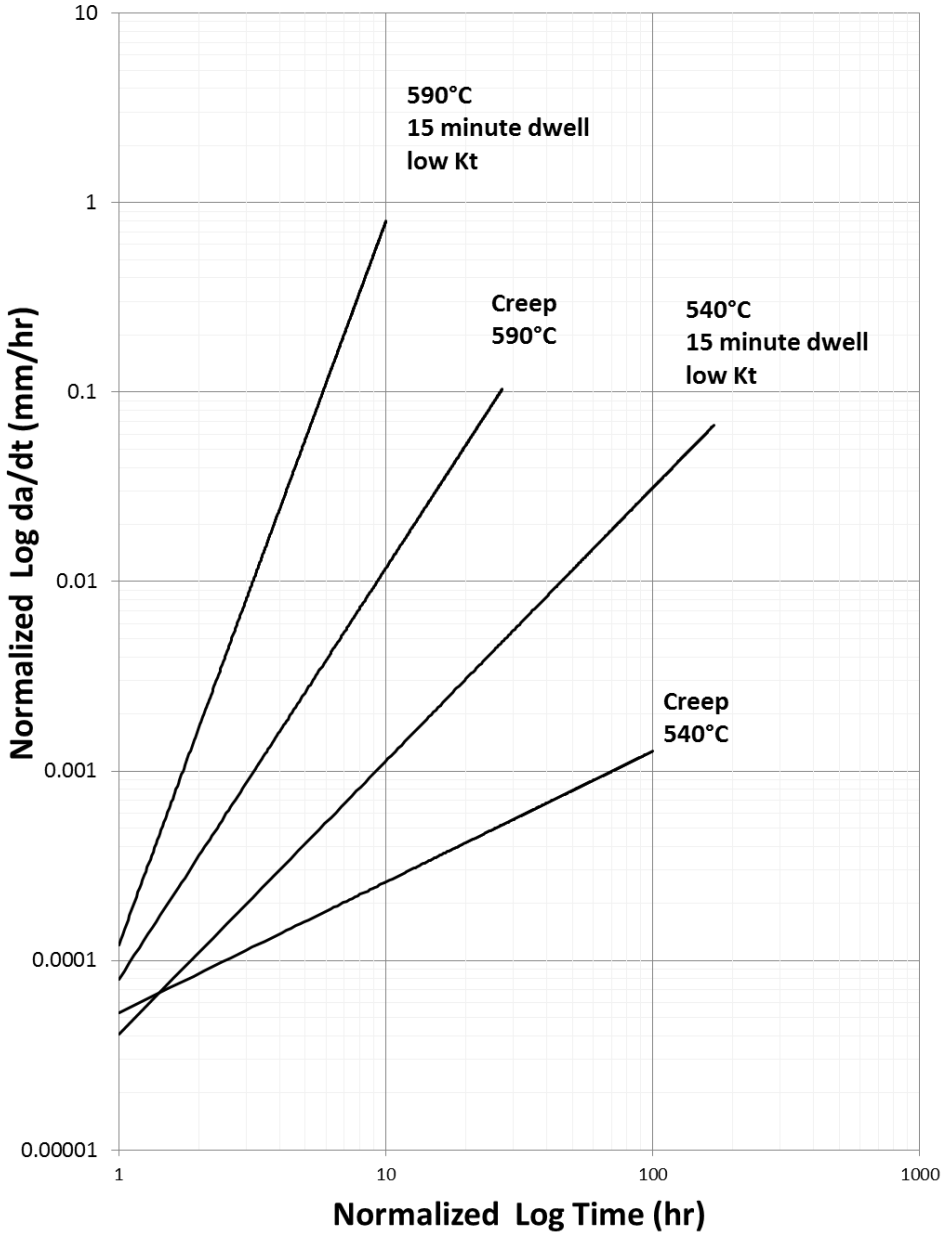

Figure 5.1 Plot of IN-718 creep crack growth testing in comparison to 15 minute dwell testing at 540°C and 590°C (low K_t)

The creep crack growth testing shows the same shift in comparison to dwell crack growth testing at both temperatures. The shallow slope for the creep crack growth data indicates a faster crack propagation rate and the steeper slope for the dwell crack growth data indicates a slower growth rate.

In addition to the crack propagation data, the fracture surfaces of the creep crack growth specimens were compared to the fracture surfaces of the time-dependent crack growth specimens. The creep crack growth specimens at both 540°C and 590°C demonstrate a clear delineation from the transgranular pre-crack to the intergranular crack propagation section, as shown in Figure 5.2.

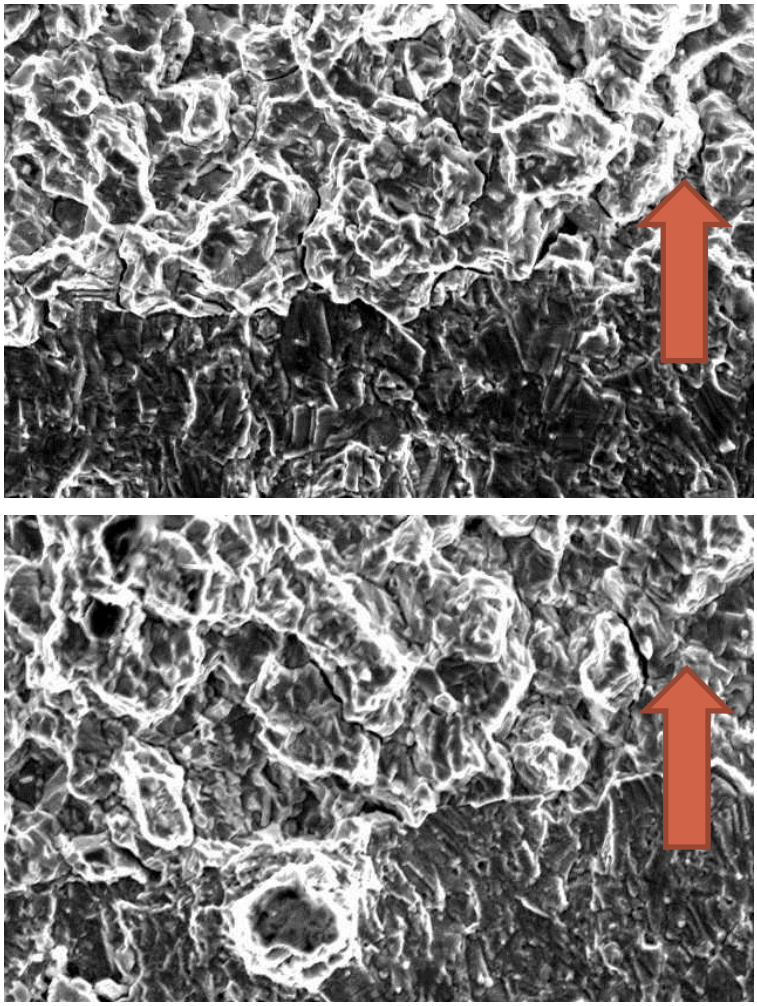

Figure 5.2 SEM images of IN-718 creep crack growth specimen at 540°C (top) and 590°C (bottom) (800X)

The transgranular and intergranular regions have distinct and clear features that differentiate between the crack mechanisms. The time dependent crack growth specimens vary between those specimens that show a clear delineation and those specimens which see multiple mechanisms in the same region. The fracture surfaces of both creep specimens are fully intergranular. Figure 5.3 shows an IN-718 specimen with a 15 minute dwell period at the 540°C with a low K_t level.

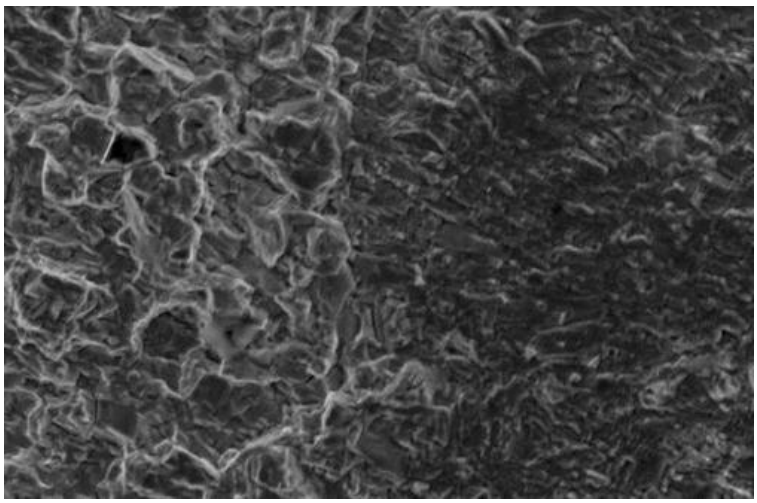

Figure 5.3 SEM image of IN-718 time dependent crack growth with 15 minute dwell period at low K_t for 540°C (800X)

Figure 5.4 shows an IN-718 specimen with a 15 minute dwell period at the 590°C with a low K_t level.

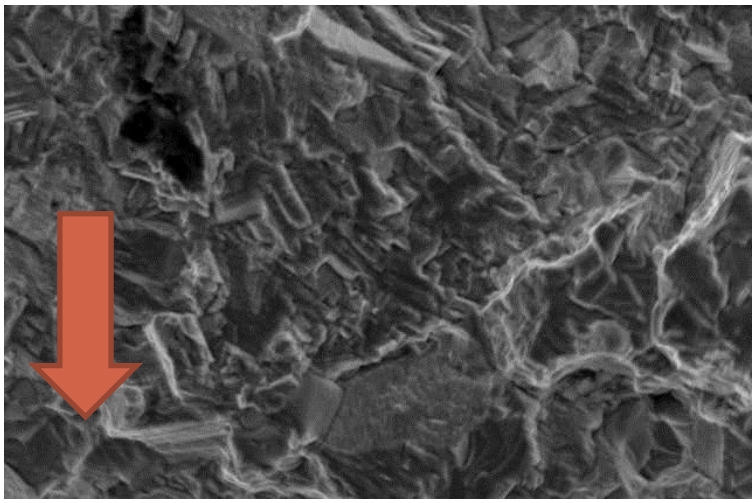

Figure 5.4 SEM image of IN-718 time dependent crack growth with a 15 minute dwell period at low K_t for 590°C (1,000X)

While the creep crack growth specimen shows a clear transition to intergranular growth, the dwell crack growth specimens at the both temperatures have a mixed mode response with striations mixing into the intergranular type structure. This mixed mode response is the most critical in that it demonstrates the transition point between two mechanisms. While the purely transgranular and purely intergranular fracture surfaces are representative of well-defined crack growth models, the mixed mode specimens also assists in indicating the way the material should be modeled under a new system.

The Waspaloy material showed a similar response to the IN-718 material in the comparison between creep crack growth results and dwell fatigue crack growth results. Three different dwell periods were applied in the Waspaloy portion of the research program: 5 minute, 15 minute, and 60 minute. All specimens had a low K_t geometry. A plot of the crack growth rate comparison at 540°C is shown in Figure 5.5 and the rate comparison at 650°C is shown in Figure 5.6. The mid-range temperature results at 590°C were very similar to the high temperature rate results.

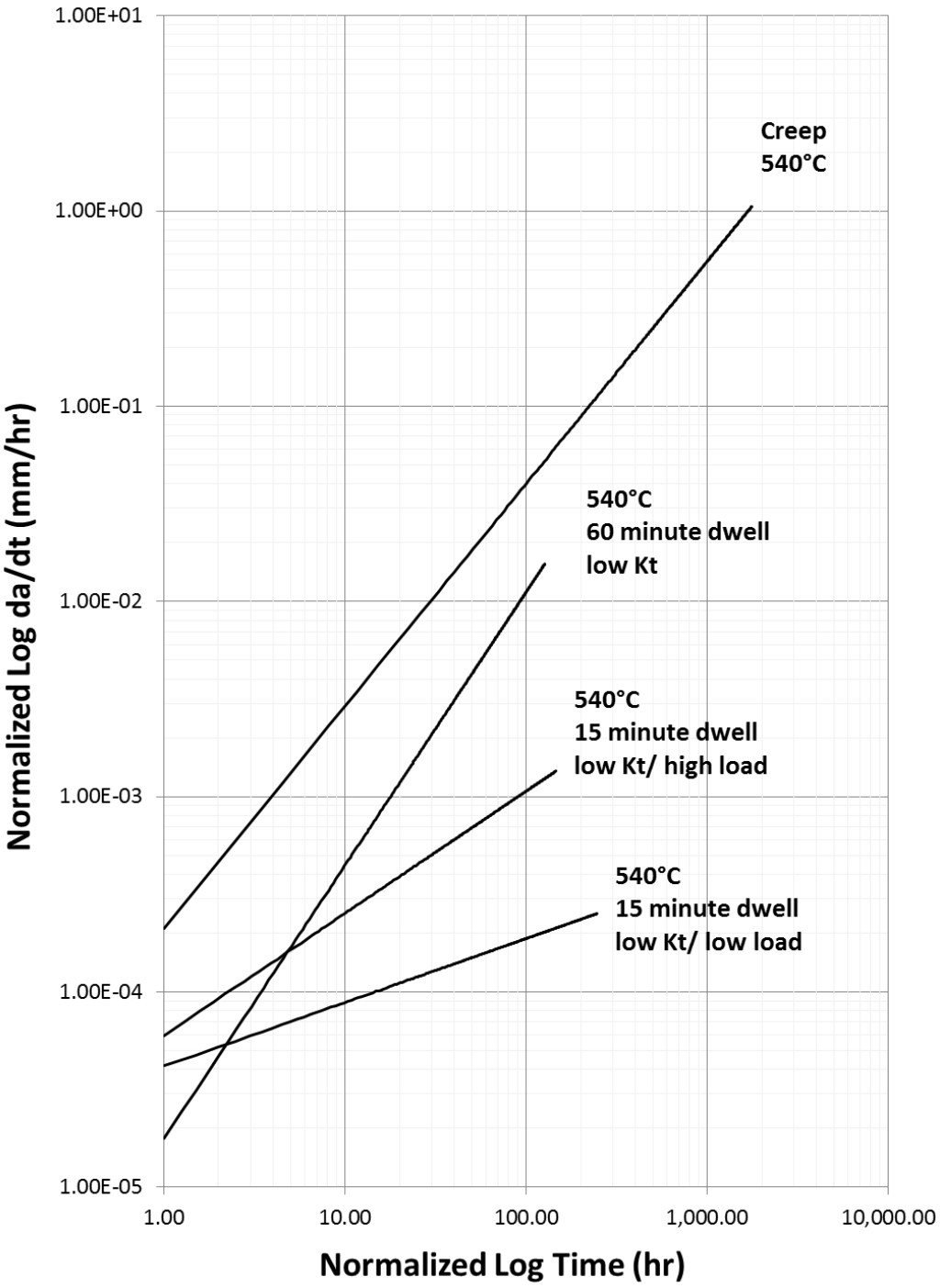

Figure 5.5 Plot of Waspaloy creep crack growth testing in comparison to dwell testing at 540°C

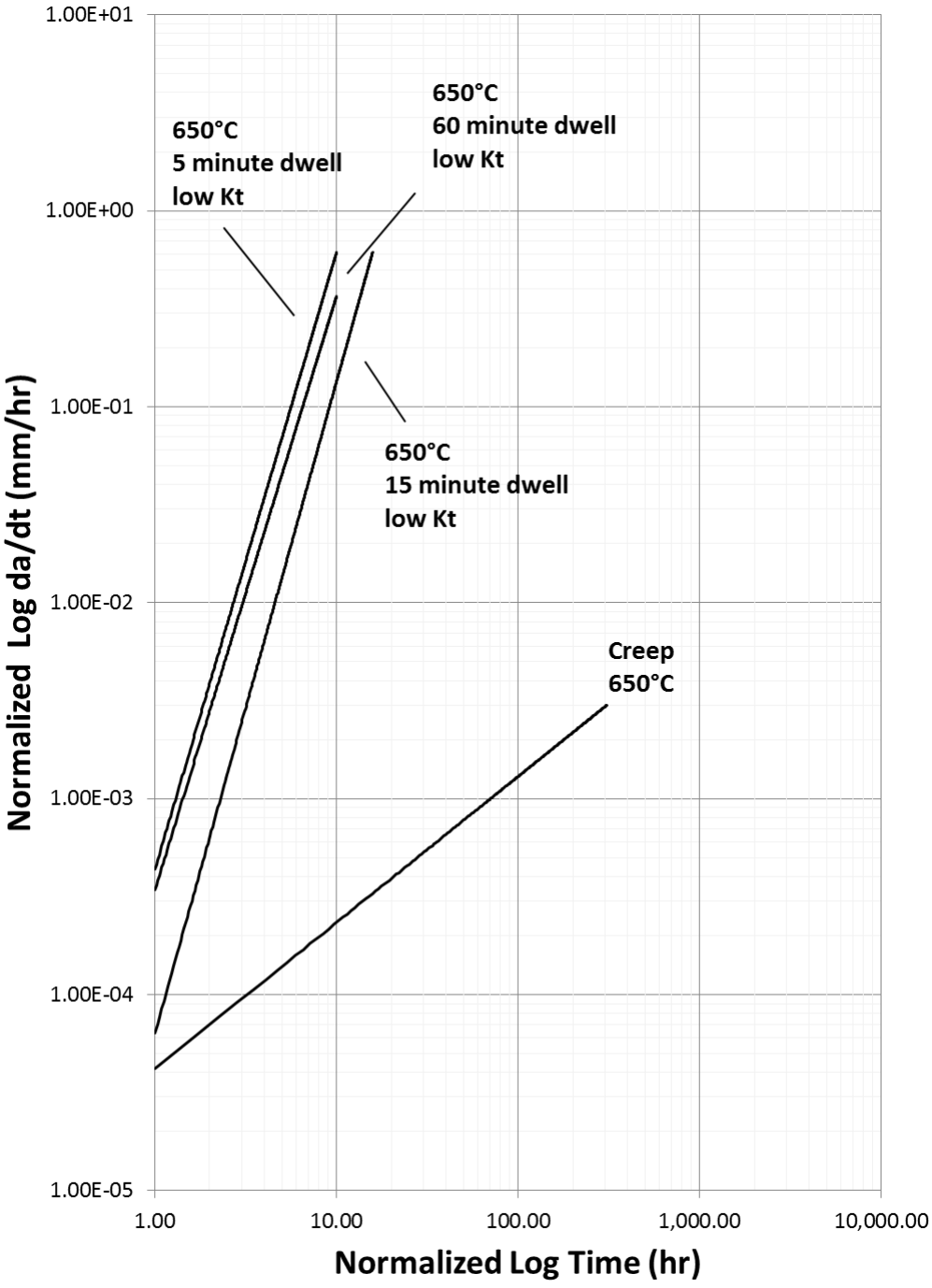

Figure 5.6 Plot of Waspaloy creep crack growth testing in comparison to dwell testing at 650°C

As shown by the trends above, the load level does not significantly affect the crack growth rate when all other conditions are held constant. The slope of the crack propagation curves are fairly consistent across all dwell times and show a similar pattern in comparison to the creep crack growth curve.

The fracture surfaces for the Waspaloy specimens under creep crack growth and under dwell crack growth conditions show very similar transition characteristics to the IN-718 results. A comparison of the two fracture surfaces for creep testing are shown in Figure 5.7.

(a)

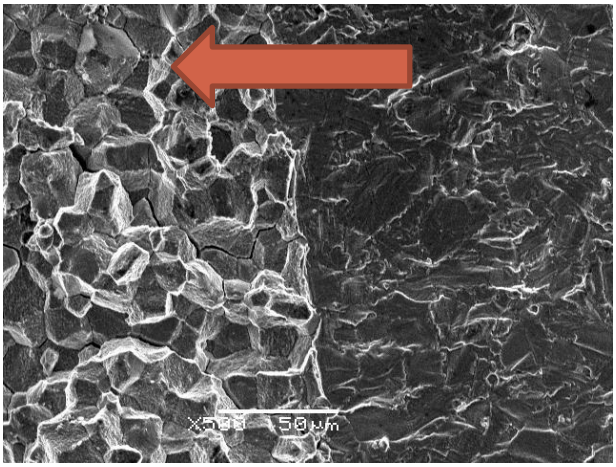

(b)

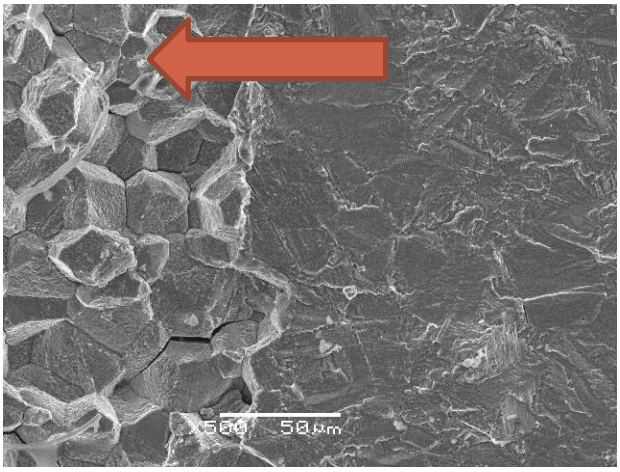

Figure 5.7 SEM images of Waspaloy creep crack growth fracture surfaces: (a) low temperature, (b) high temperature

The fracture morphology is representative of a classical switch from a transgranular pre-crack to an intergranular crack progression. The intergranular structure has a blocky structure and some clear signs of secondary cracking which is characteristic of time dependent crack growth.

The dwell crack growth testing for Waspaloy has a more mixed mode response. The 15 minute dwell fracture surface is shown in Figure 5.8 while the 60 minute dwell fracture surface is shown in Figure 5.9.

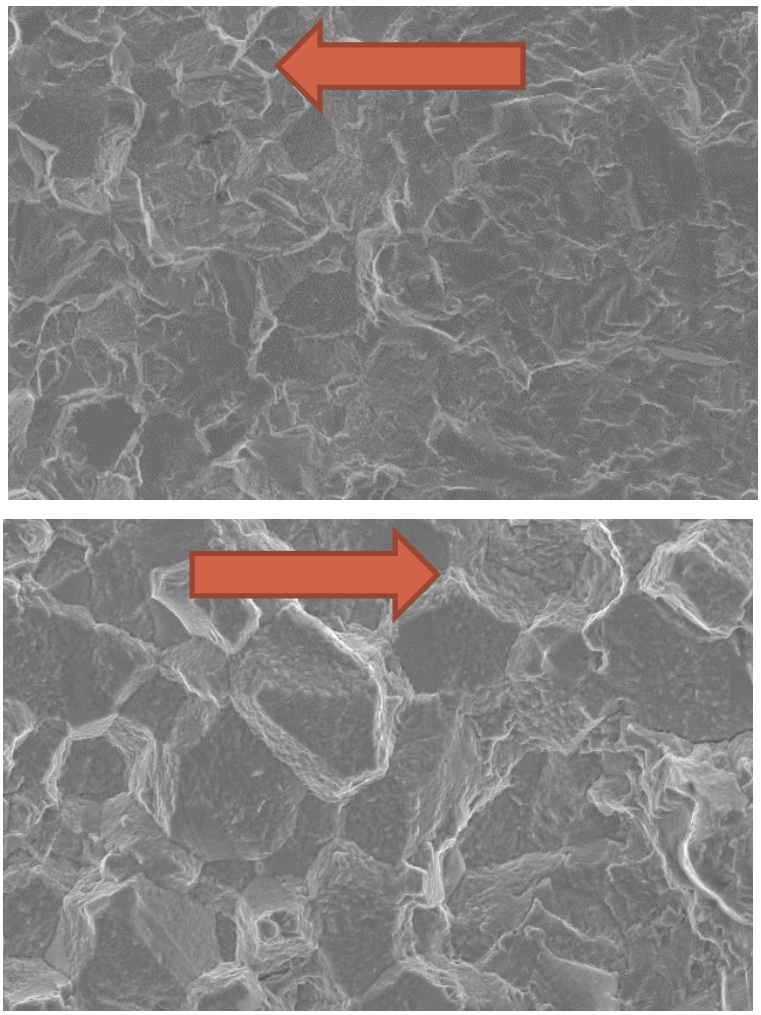

Figure 5.8 SEM images of Waspaloy time dependent fatigue crack growth fracture surface at 540°C for a 15 minute dwell period at a low K_t. The top image (500X) is for low applied load and the bottom image (1000X) is for high applied load.

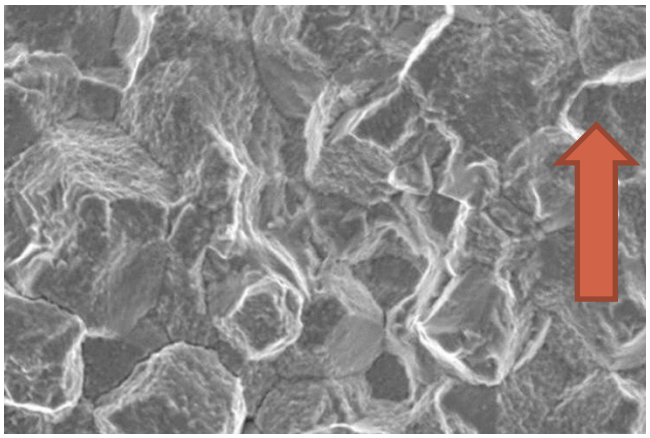

Figure 5.9 SEM image of Waspaloy time dependent fatigue crack growth fracture surface at 540°C for a 60 minute dwell period at low K_t (1,000X)

As the dwell period increases, the amount of intergranular fracture surface features increases. The Waspaloy fracture surfaces have the appearance of a smooth finish in comparison to the IN-718 fracture surfaces. These images help clarify the difference between pure transgranular and intergranular regions for comparison with the mixed mode fracture surfaces.

The fracture surfaces associated with high temperature dwell crack growth testing are all fully transitioned from a transgranular pre-crack region to a fully intergranular crack progression. There is some evidence of secondary cracking in the intergranular regions at all three temperatures tested. This high temperature SEM results show the same trends as the mid-range temperature fracture surfaces. The high temperature fracture surfaces are shown in Figure 5.10 to Figure 5.11 with 5 minute, 15 minute, and 60 minute dwell respectively.

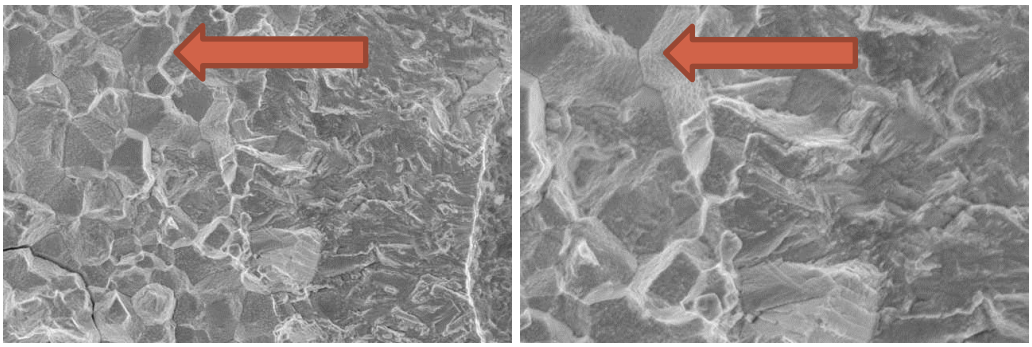

Figure 5.10 SEM images of Waspaloy dwell fatigue crack growth at 5 minute dwell period (low K_t, 650°C)

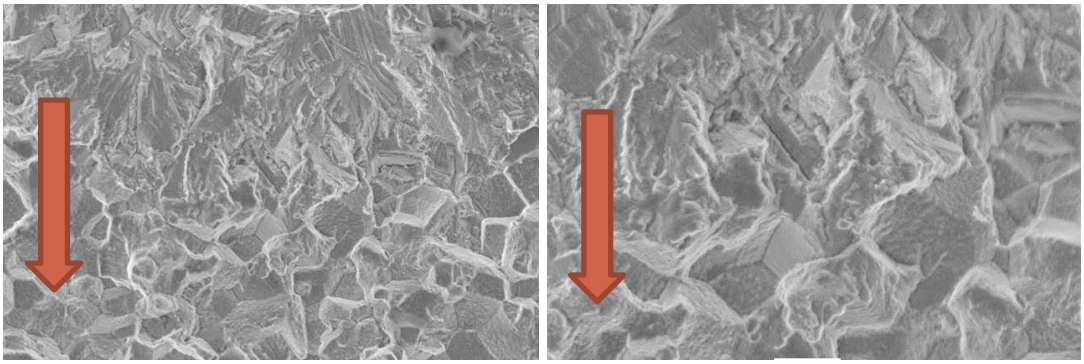

Figure 5.11 SEM images of Waspaloy dwell fatigue crack growth at 15 minute dwell period (low K_t, 650°C)

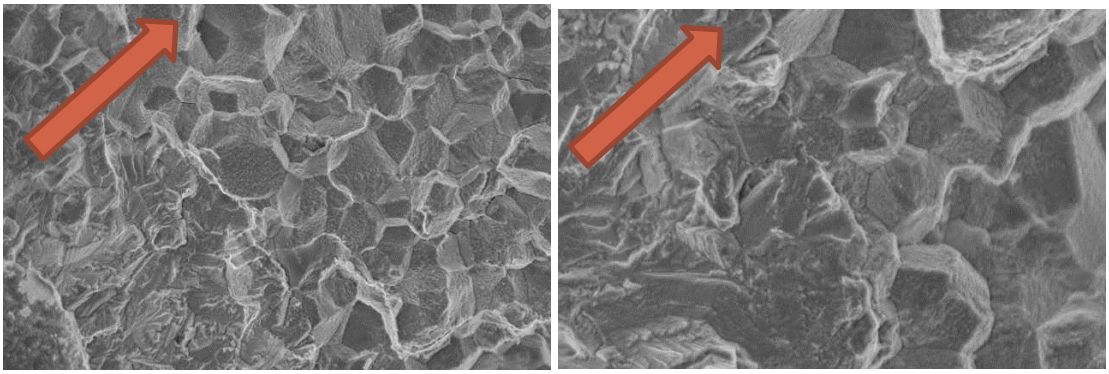

Figure 5.12 SEM images of Waspaloy dwell fatigue crack growth at 10 minute dwell period (low K_t, 650°C)

The increase in temperature made the Waspaloy material more likely to transition and increases the amount of intergranular features. An increase in the applied load had a similar effect on the transition results. This indicates that a lower load level or dwell period would be required to increase the number of mixed mode conditions for this alloy.

5.2 Geometry

The effect of geometry on crack growth rates and fracture surface is one of the major tenants of the research program. All three materials were tested at different geometries. A plot of the crack propagation rate associated with the different geometry values is shown in Figure 5.13.

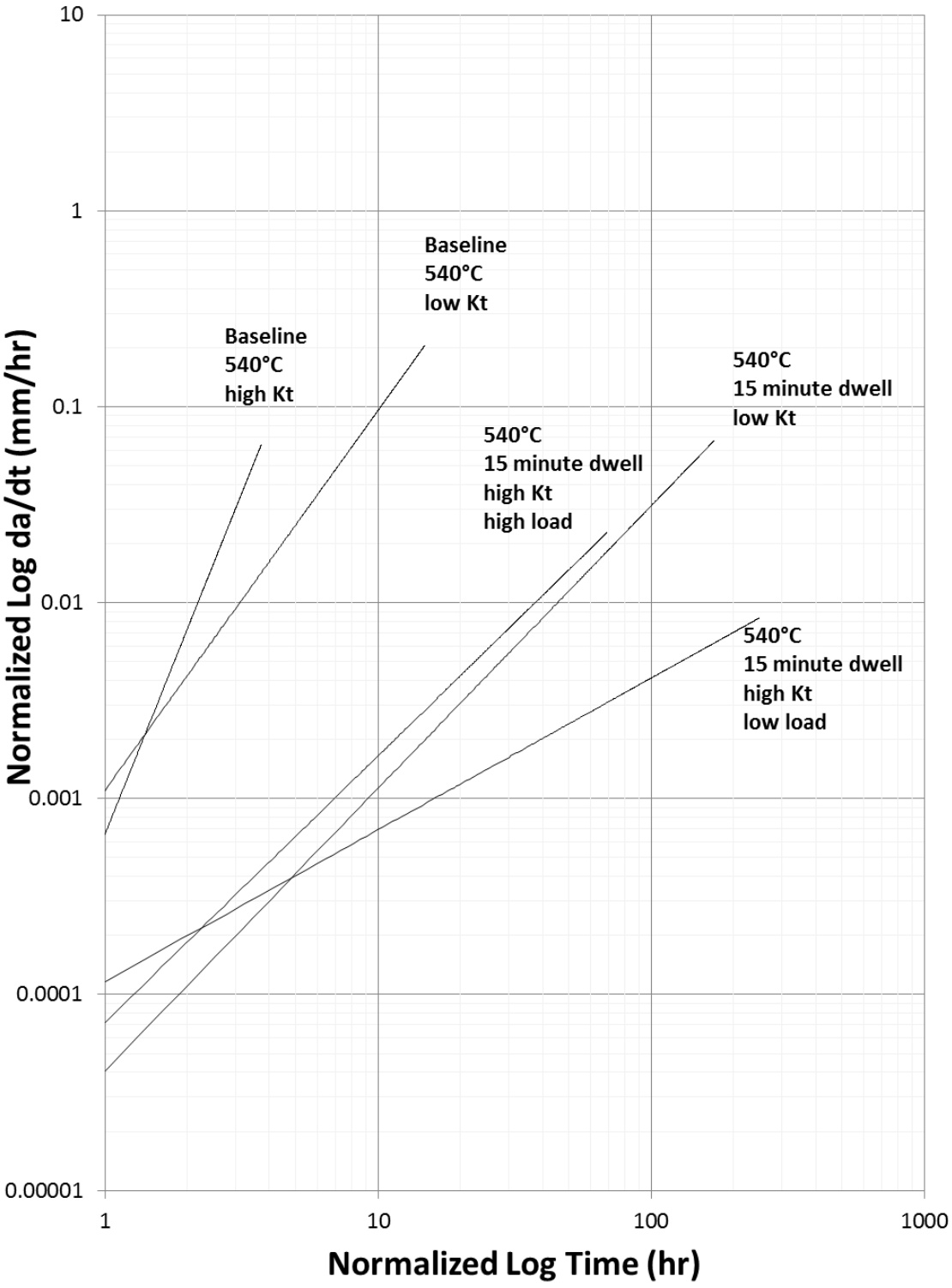

Figure 5.13 Plot of IN-718 dwell crack growth testing at 540°C at various geometries and load levels

The crack propagation results indicate that there is a limited difference in crack propagation rate between the low and high K_t level. There is a clear shift that occurs between the baseline testing and the specimens which have a K_t notch geometry. The baseline testing has a faster crack propagation rate compared to the dwell crack growth testing.

The fracture surface associated with these K_t values demonstrates the transition between transgranular and intergranular crack progression. The baseline test specimen has a transgranular fracture surface which is consistent with a cycle dependent crack growth test. The fracture surface of the low K_t and low load specimen are shown in Figure 5.14.

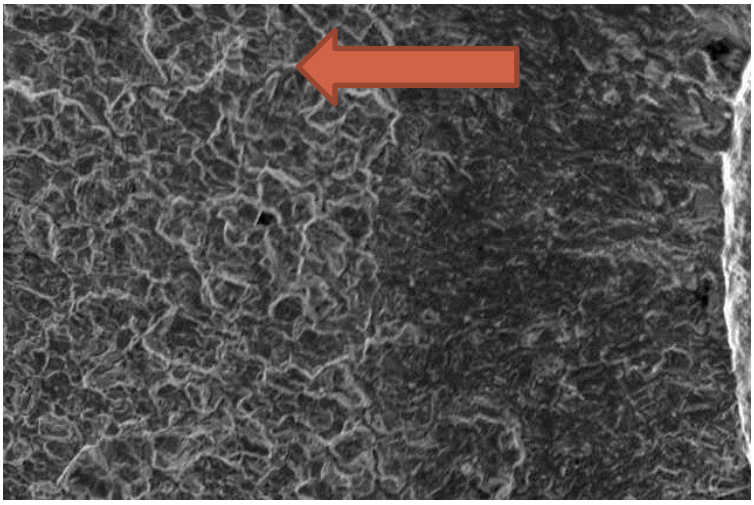

Figure 5.14 SEM images of IN718 low K_t dwell fatigue crack growth specimen at 540°C and 15 minute dwell (400X)

The fracture surface has a relatively small level of mixed mode characteristics, where there are some transgranular features included in the intergranular region. A SEM image from the high Kt specimen are shown in Figure 5.15.

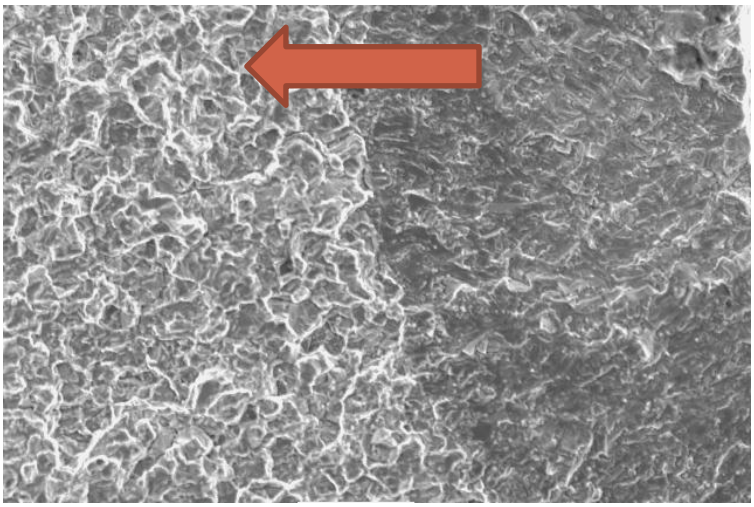

Figure 5.15 SEM image of IN718 high K_t, low load dwell fatigue crack growth specimen at 537.8°C (400X)

The high K_t geometry fracture surface has a clear transition from the transgranular pre-crack region to the intergranular crack progression with a very small amount of transgranular features.

Multiple specimen geometries were also tested for Waspaloy material at various notch K_t levels. The low K_t specimen was tested both at a low load level and a high load level to help determine whether the geometry or the load level has a greater effect on the crack propagation rate. A plot of the crack growth rates is shown in Figure 5.16.

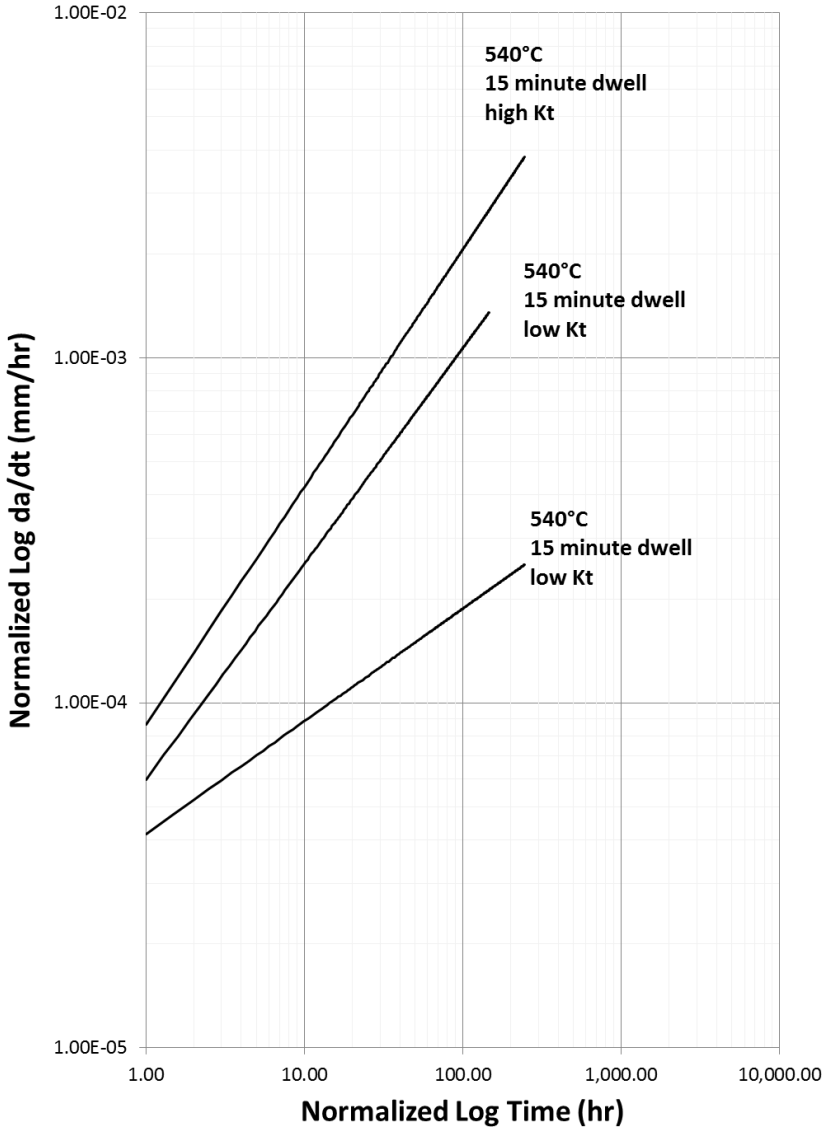

Figure 5.16 Plot of Waspaloy time dependent crack growth at a variety of notch geometries under 15 minute dwell period (540°C, low K_t)

A plot of the Waspaloy crack growth results also indicates that the crack growth rate increases slightly as the notch K_t increases. The low load level has a slightly slower crack growth rate in comparison to the high load level of the same geometry.

The fracture surfaces associated with these test results also demonstrate a spectrum of crack growth behavior at different geometries. The SEM images associated with a low K_t notch geometry are shown in Figure 5.17.

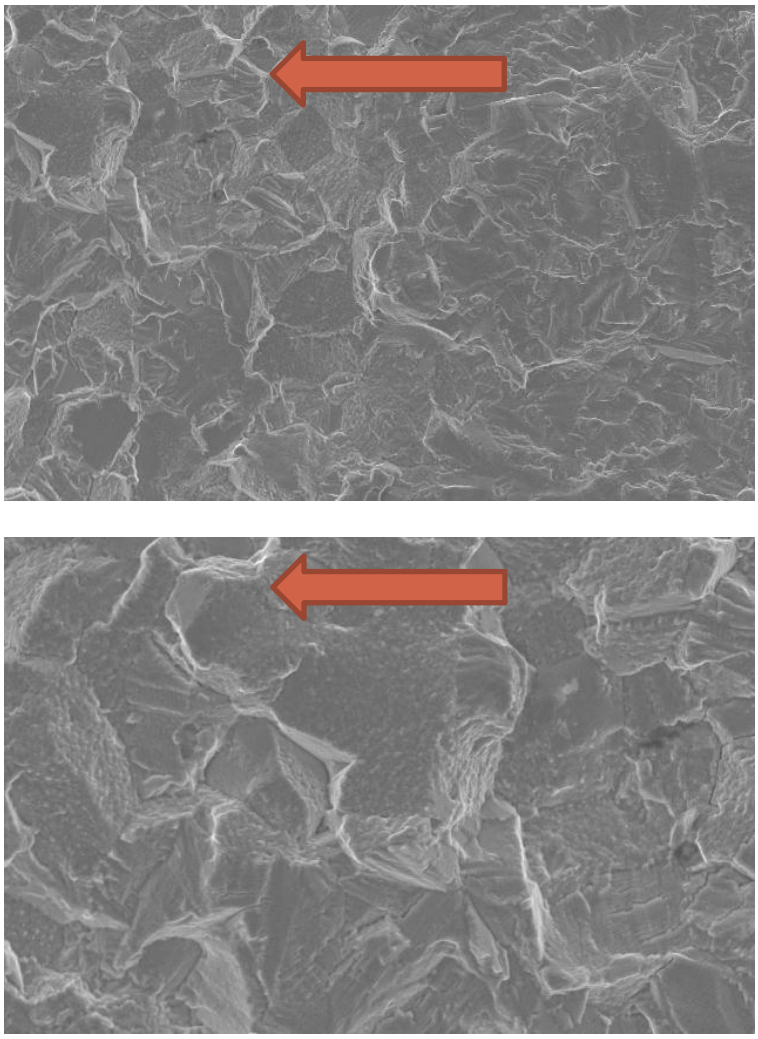

Figure 5.17 SEM images of the Waspaloy dwell crack growth fracture surface for the low K_t Kb bar specimens and 15 minute dwell period. The top image shows low magnification (500X) and the top image shows high magnification (1,000X).

The low K_t notch geometry has fracture surface features that are consistent with a mixed mode crack progression. There are both blocky structures which are attributed to intergranular crack growth and there are intermixed striations which are attributed to transgranular crack growth. Out of the three temperatures tested for Waspaloy material, this temperature was also the lowest of the three evaluated. Therefore the low K_t geometry and the low temperature combine to ensure that this test condition did not fully transition to time dependent crack growth behavior.

The SEM image associated with the high K_t geometry specimen for the Waspaloy material is shown in Figure 5.18.

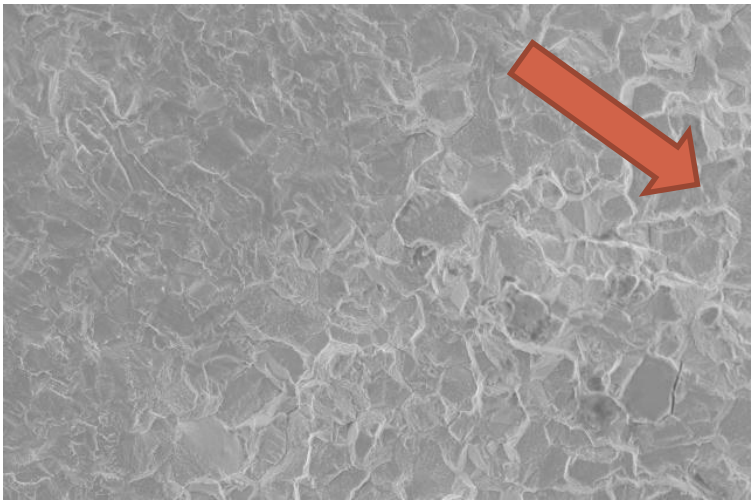

Figure 5.18 SEM image of Waspaloy dwell fatigue crack growth with a high K_t and a 15 minute dwell period (400X)

The fracture surface associated with the high K_t geometry shows a clear transition from transgranular to intergranular crack progression. The higher K_t geometry created a region of more concentrated stress near the crack and performed differently than the low K_t geometry. The fracture surfaces were consistent between the low and high load levels for this material.

The notch geometry was also evaluated for U-720 material. A plot of the crack growth rate results are shown in Figure 5.19. All specimens were tested at 650°C with a 15 minute dwell period.

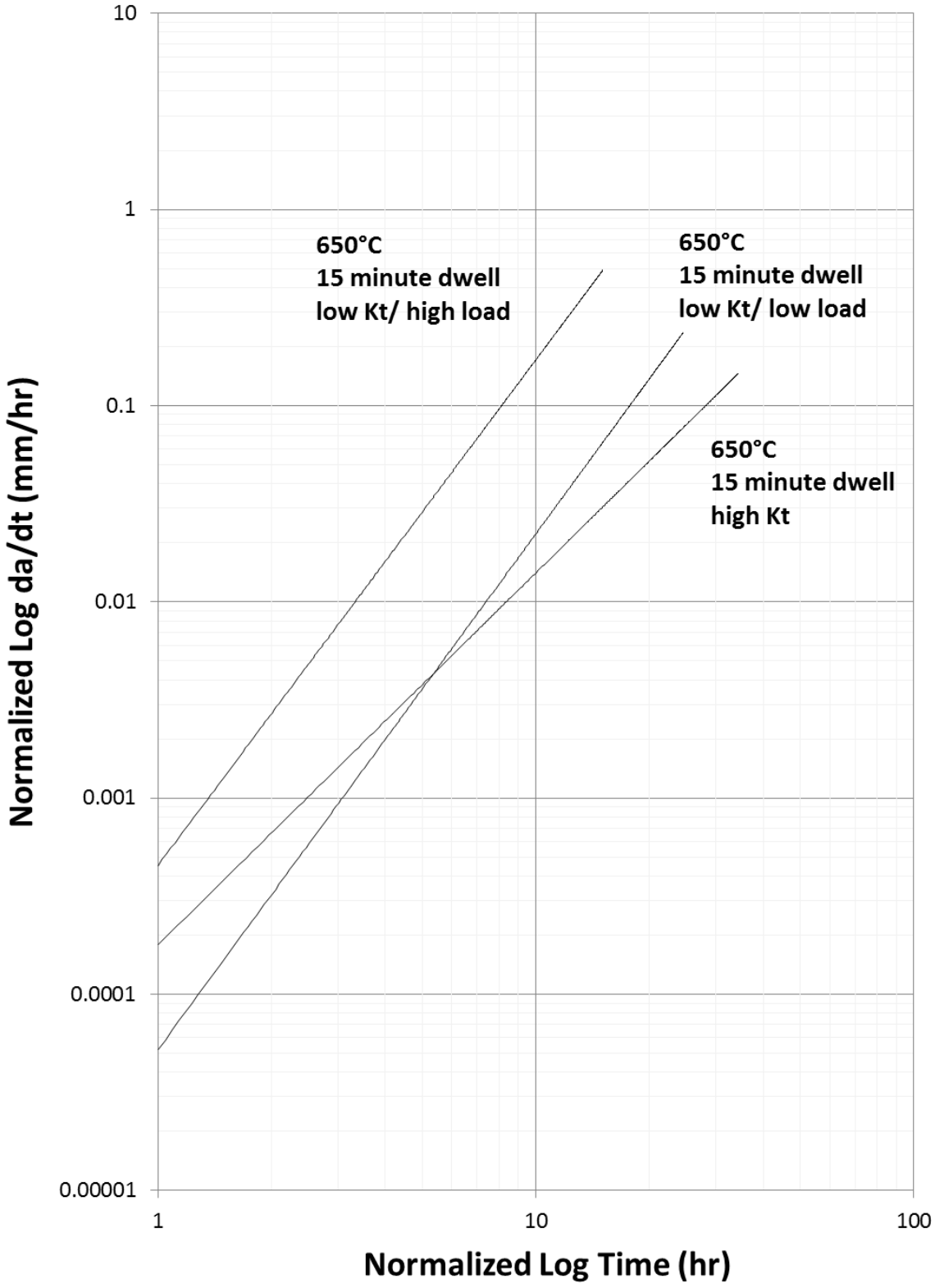

Figure 5.19 Plot of U-720 material time dependent fatigue crack growth at different notch geometries under 15 minute dwell period (650°C)

The U-720 results show little change in crack growth rate between low and high K_t values. Unlike the IN718 and Waspaloy results, there is no change in slope for the crack growth curve that would indicate that geometry has an influence on the material response. The low applied load had a slightly different slope compared to the high applied load test result.

The fracture surface of the corresponding specimens demonstrated that all of the U-720 specimens were consistent with time dependent fatigue crack growth behavior. The SEM images are shown in Figure 5.20 and Figure 5.21.

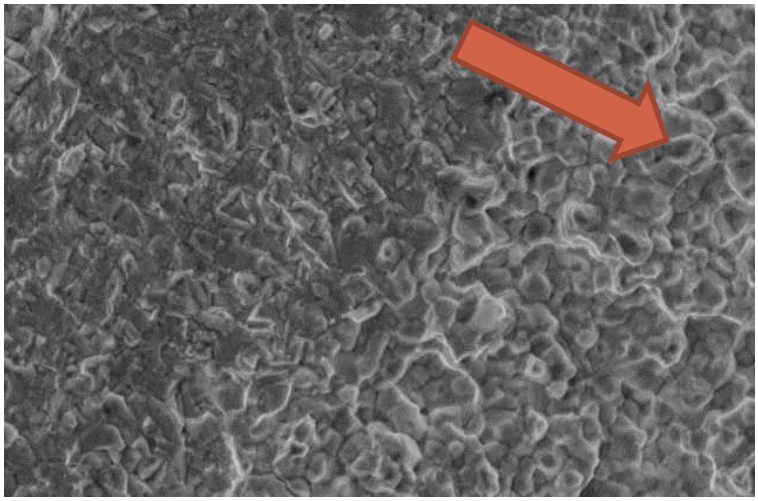

Figure 5.20 SEM images of Waspaloy material at low K_t notch geometry (800X)

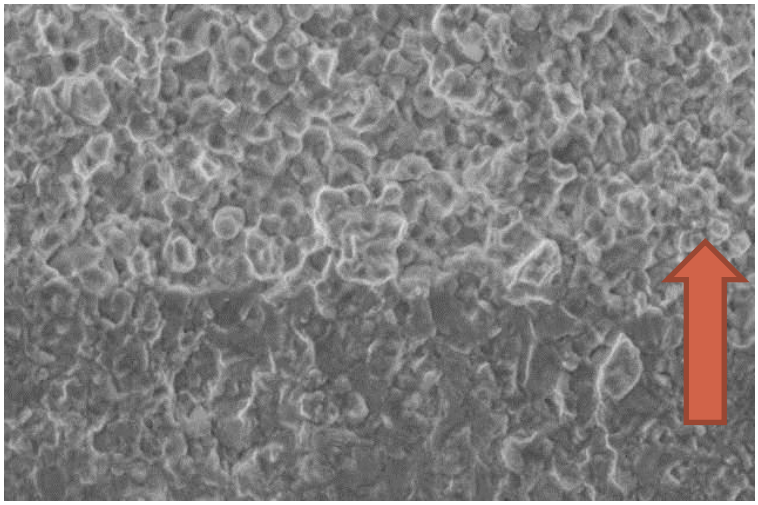

Figure 5.21 SEM images of Waspaloy material at high K_t notch geometry (800X)

The fracture surfaces of the low and high K_t crack growth specimens showed a very similar transition from transgranular pre-crack to intergranular time dependent crack progression. The combination of temperature and geometry for U-720 material cause the material to operate under fully time dependent conditions.

5.3 Temperature

All three materials were tested across a small temperature range to capture each material both above and below the expected dwell transition temperature. The goal was to see how small temperature ranges affect the crack propagation rate and transition point on the fracture surfaces.

For IN-718, the material was tested at 470°C, 540°C, and 590°C. A comparison of the crack growth rates at various temperatures was shown in Figure 5.22. All specimens were tested at a low K_t value and at a 15 minute dwell period. The expectation is that the crack growth rate increases as the temperature increases while the rest of the test parameters are held constant.

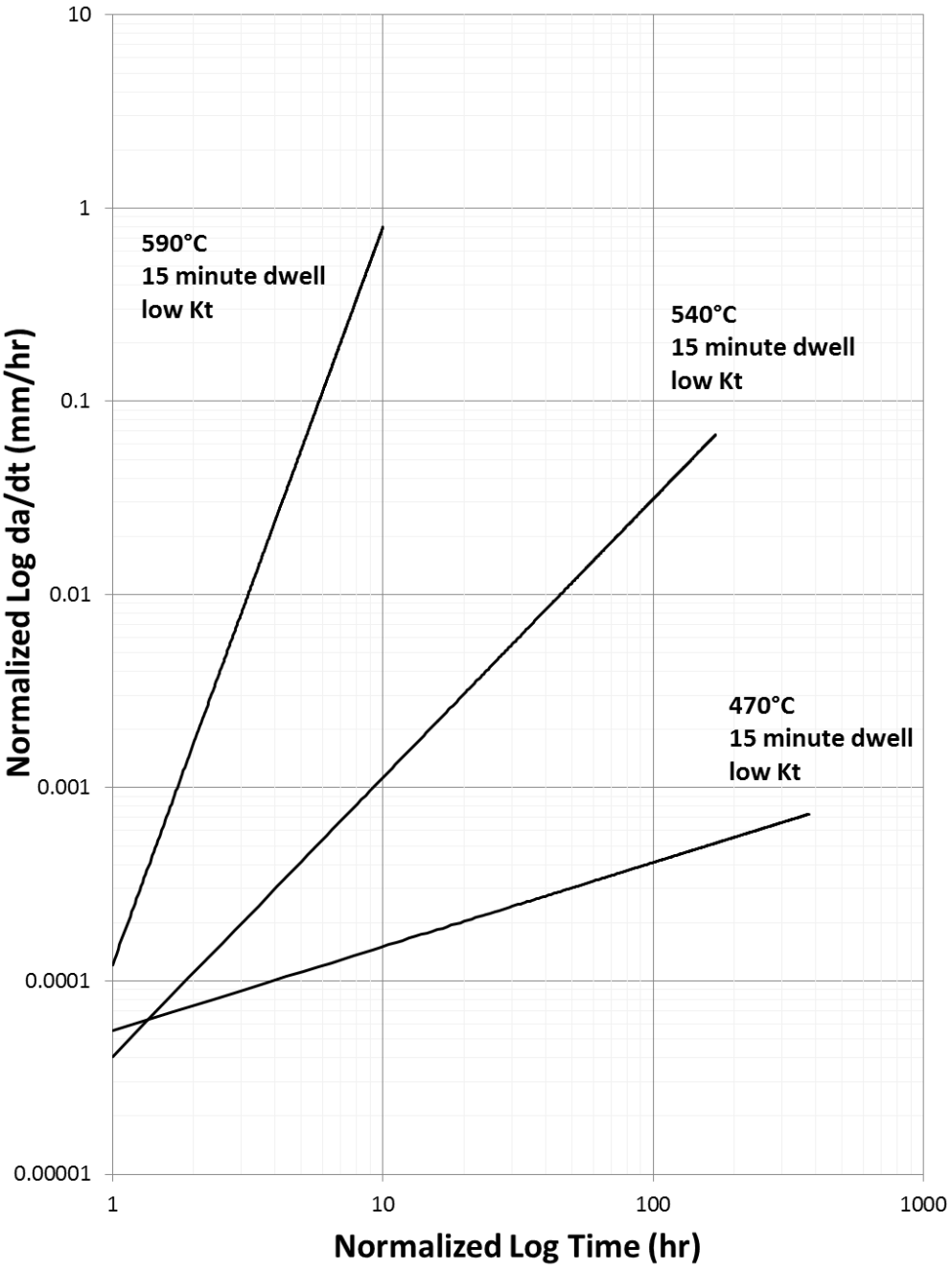

Figure 5.22 Plot of IN-718 time dependent fatigue crack growth at different temperatures (low K_t, 15 minute dwell period)

The plot of the data demonstrates that the crack growth rate increases as the temperature increases. The change in slope is incremental with the corresponding temperature changes.

The fracture surfaces that correspond with these results show that show a variety of crack mechanisms. SEM images of the IN718 fracture surfaces across the temperature range are shown in Figure 5.23, 5.24, and 5.25.

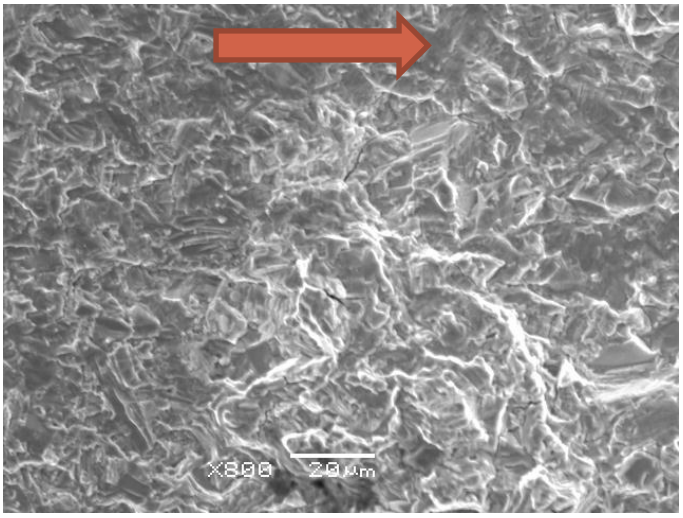

Figure 5.23 SEM image of IN-718 dwell crack growth at 470°C low K_t and a 15 minute dwell period (800X)

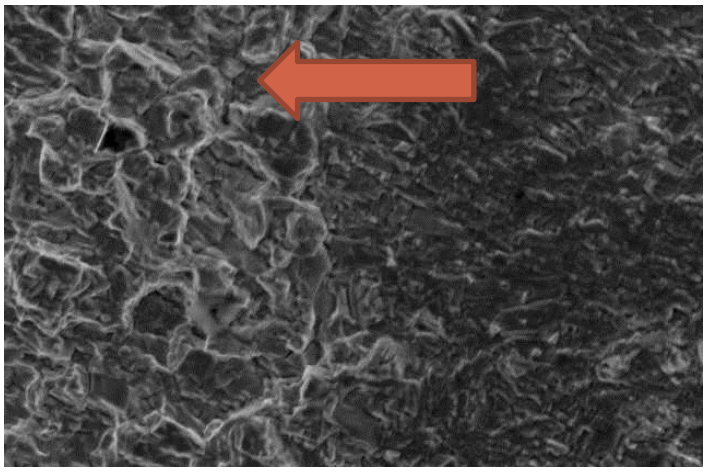

Figure 5.24 SEM image of IN-718 dwell crack growth specimen at 540°C low K_t and a 15 minute dwell period (800X)

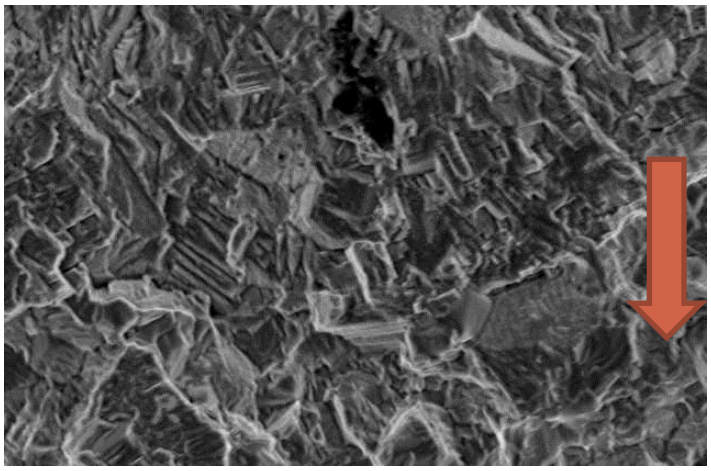

Figure 5.25 SEM images of IN718 material at the 590°C low K_t and a 15 minute dwell period (800X)

The fracture surface images demonstrate that all three temperatures have some mixed mode fracture surface characteristics. The high temperature fracture surface shows the least amount of striations and does represent time dependent crack growth.

5.4 Load Sequence

Waveform testing on Waspaloy material was performed to demonstrate the effects of altering the waveform in the middle of a test cycle. As mentioned in the procedure, the test started off with a pre-crack followed by a dwell crack growth cycle for a set time period. After a set period of time, the waveform was changed to a triangular waveform with no dwell period. After another period of time, the trapezoidal dwell cycle was re-initiated. The discontinuous waveform was tested at 540°C or the low temperature for Waspaloy. While the change in waveform did not affect the crack propagation rate, the fracture surface did display evidence of the change in mission. The SEM images of the fracture surface are shown in Figure 5.26.

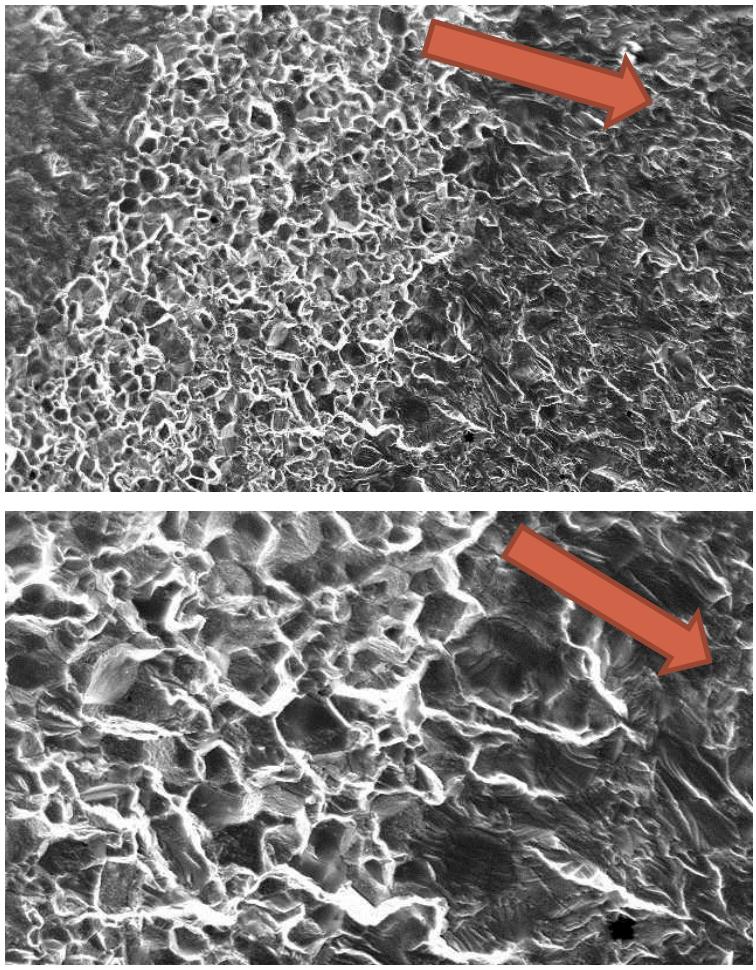

Figure 5.26 SEM images of the Waspaloy baseline specimen tested with a discontinuous waveform. The top image is at low magnification (150X) and the bottom image is at high magnification (400X)

The images demonstrate that the crack started with a transgranular pre-crack region followed by an intergranular crack growth region associated with the dwell period. When the dwell load is removed and the triangular load is applied, the crack path switches back to transgranular appearance. As the dwell cycle is re-applied, the fracture pattern switches back to an intergranular path for the remainder of the crack growth across the specimen. This indicates that the specimen followed the predicted behavior patterns.

The overload condition was evaluated on IN-718 to determine how the mission will affect the crack growth rate and the corresponding fracture surface. The load level was varied in two different overload tests to quantify the difference

between a higher and lower overload level. The lower overload level was 105 % of the dwell load level. The higher overload level was 120% of the dwell load level. The fracture surface results at low temperature which correspond to these test results demonstrate that the overload testing transitioned from a transgranular pre-crack to an intergranular crack path for a short period of time. After a while, the crack returned to a transgranular path. The SEM images for low temperature IN-718 overload testing are shown in Figure 5.27.

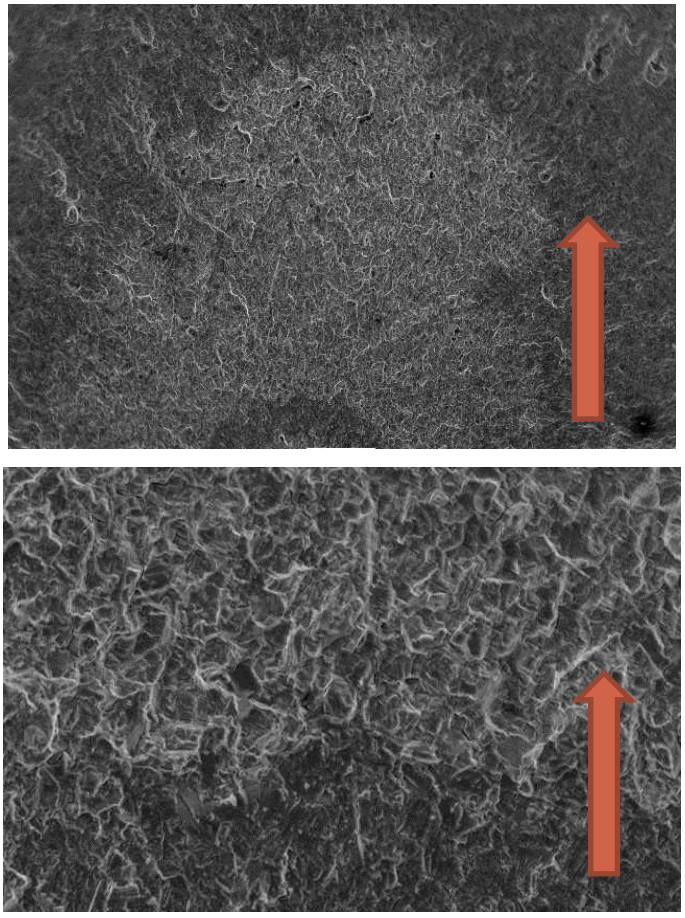

Figure 5.27 SEM images of time dependent IN718 crack growth samples with an overload cycle at 540°C. The top image is at low magnification (65X) and the bottom image is at high magnification (400X).

The top image suggests that the high K_t specimens goes through a transgranular pre-crack, an intergranular mixed mode region, and a transition back to transgranular crack growth rate. This indicates that the geometry may force the

time dependent effect to relax back out of the specimen at longer test times with an initial overload applied. The fracture surfaces of the low and high overload specimens were very similar in appearance which is expected based on the crack propagation data. The SEM images for IN-718 overload testing at 590°C high temperature with a low overload level are shown in Figure 5.28.

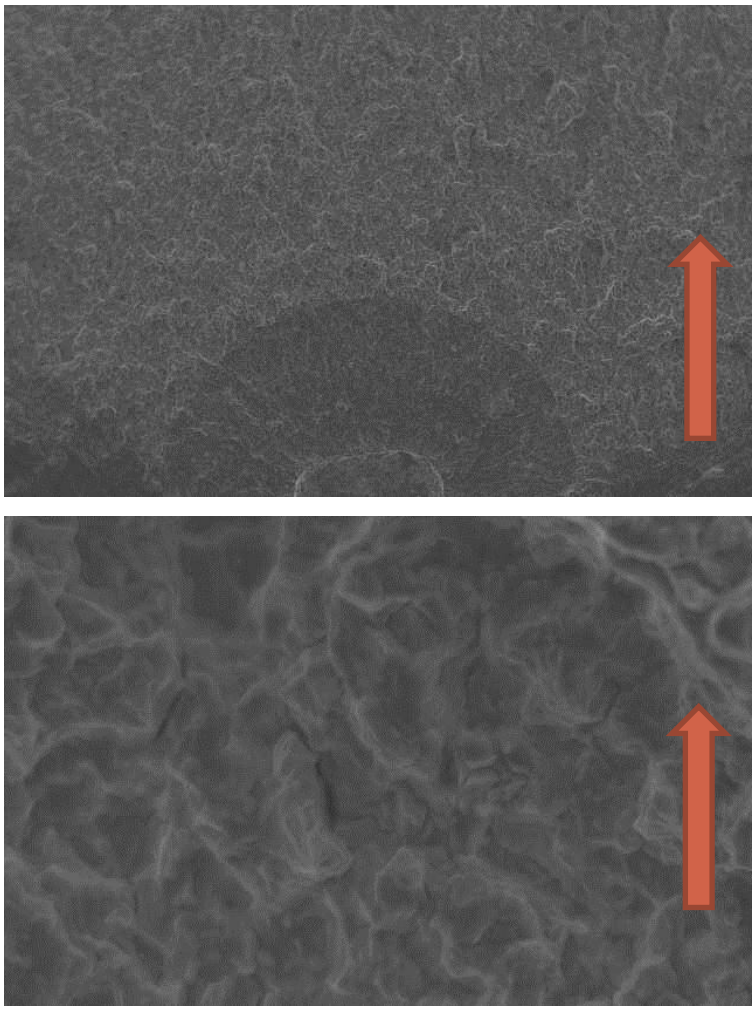

Figure 5.28 SEM images of time dependent IN-718 crack growth fracture surfaces with an overload cycle at 590°C. The top image is taken at low magnification (100X) and the bottom images is taken at high magnification (1,500X).

The fracture surface has a transgranular pre-crack region followed by an intergranular crack growth region across the rest of the crack path. Unlike the intermediate temperature testing, the high temperature testing does not relax back out of the intergranular region after a set period of time. The SEM images for IN-718 overload testing at 590°C high temperature with a high overload level show the same behavior and are shown in Figure 5.29.

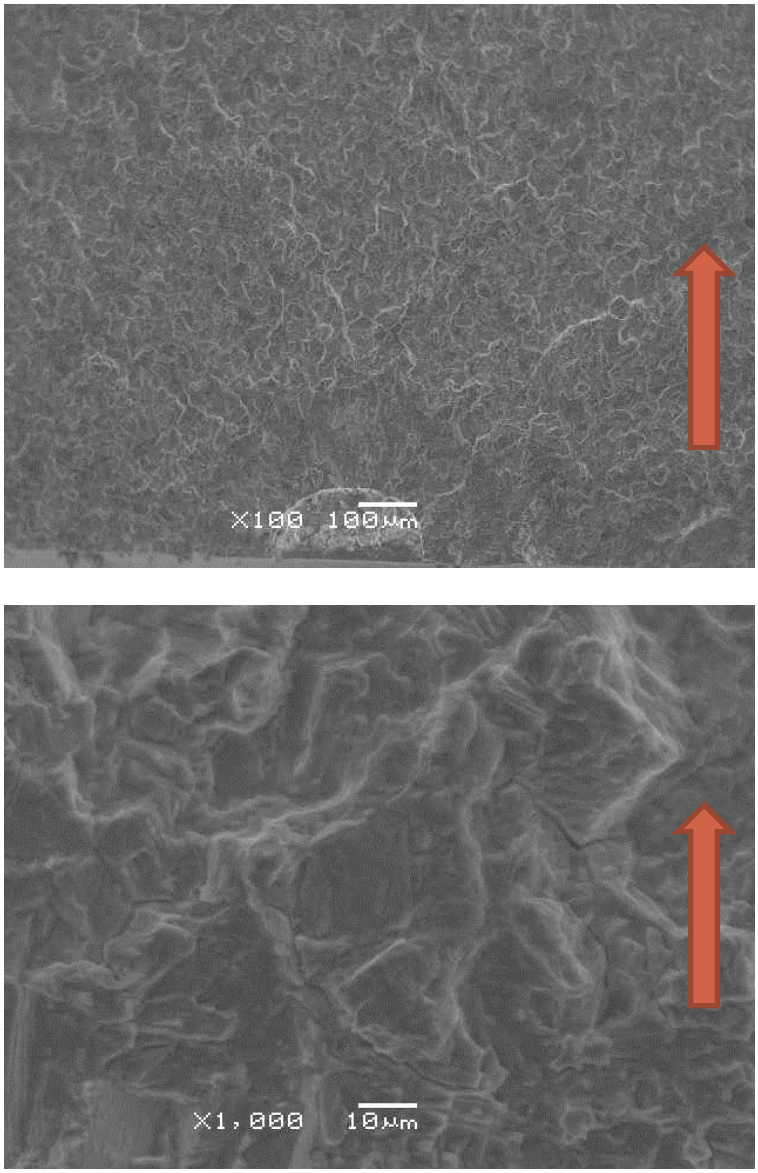

Figure 5.29 SEM images of time dependent IN-718 crack growth samples with an overload cycle at 590°C. The top image is taken at low magnification (100X) and the bottom images is taken at high magnification (1,500X).

The high temperature overload fracture surfaces both have high levels of secondary cracking which indicates a more violent crack growth pattern. The overload specimens have the highest level of competing mechanisms between overload and time dependent effects trying to occur simultaneously.

5.5 Materials

Material was removed from the three forgings at both the rim and hub locations. In order to determine how much the microstructure fluctuates between these two locations in each material, a microstructural sample was procured from each location and evaluated. The test temperatures are not high enough to cause any microstructural changes to the material, so these images will serve to document the material condition both before and after test. The IN-718 microstructural images are shown in Figure 5.30 and Figure 5.31.

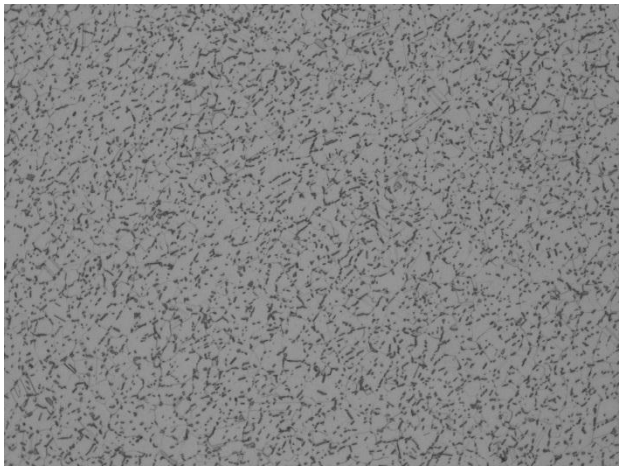

Figure 5.30 IN-718 microstructure at the forging rim location (500X)

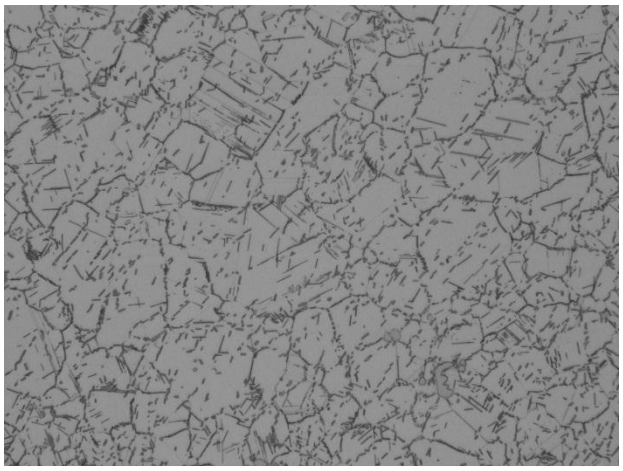

Figure 5.31 IN-718 microstructure at the forging web location (100X)

The microstructure at the rim is consistently finer than the grain size at the web location. The Waspaloy microstructural images are shown in Figure 5.32 and Figure 5.33.

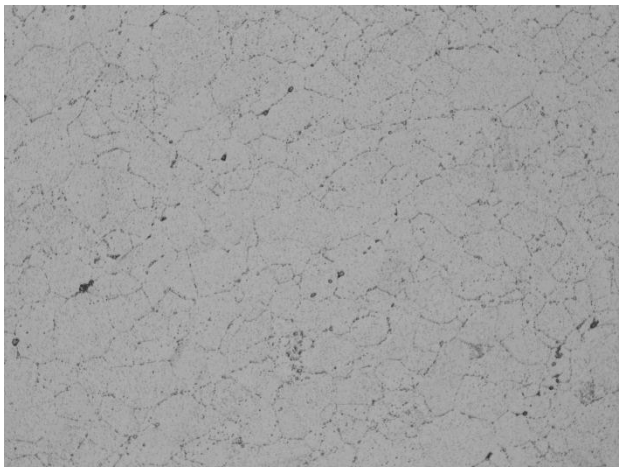

Figure 5.32 Waspaloy microstructure at the forging rim location (500X)

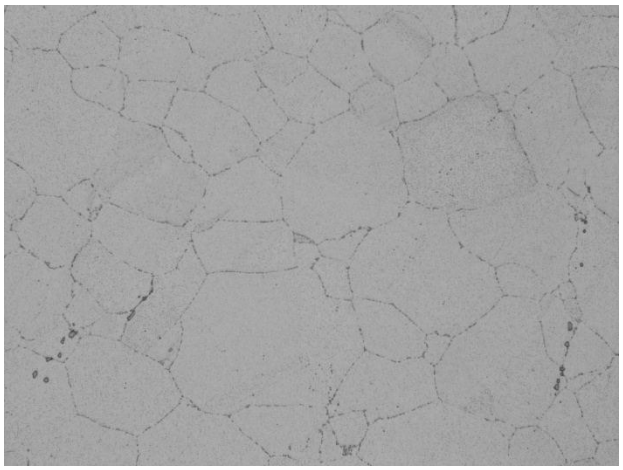

Figure 5.33 Waspaloy microstructure at the forging web location (500X)

Similar to the IN-718 material, the grain size at the rim is consistently finer than the web location. The U-720 microstructural images are shown in Figure 5.34 and Figure 5.35.

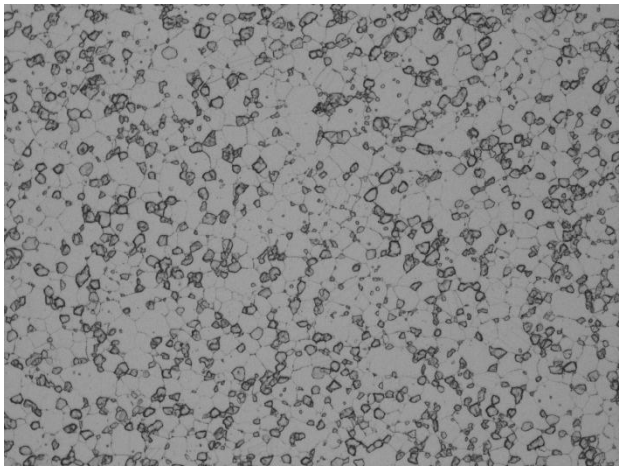

Figure 5.34 U-720 microstructure at the forging rim location (100X)

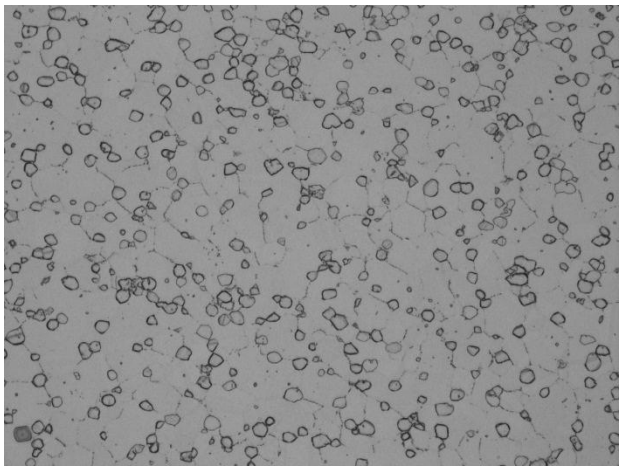

Figure 5.35 U-720 microstructure at the forging web location (500X)

The U-720 material images indicate a less distinct difference between the rim and web locations in comparison to the Waspaloy and IN-718 material, but there is still a visible change in the delta levels. In terms of grain size, the Waspaloy material has the largest average grain size (ASTM 9), IN-718 material has an intermediate average grain size (ASTM 10.5), and the U-720 material has the largest average grain size (ASTM 11.5).

A comparison plot was made for all three materials at the same test conditions in order to determine the effect of material composition and grain size. All three alloys being compared were tested at 590°C, a low K_t notch geometry, and a 15 minute dwell period. The fracture surfaces associated with these crack growth curves demonstrated that all three test specimens transition from a transgranular pre-crack region to either a mixed mode or an intergranular crack progression. A plot of the time dependent crack growth for IN-718, U-720, and Waspaloy is shown in Figure 5.36.

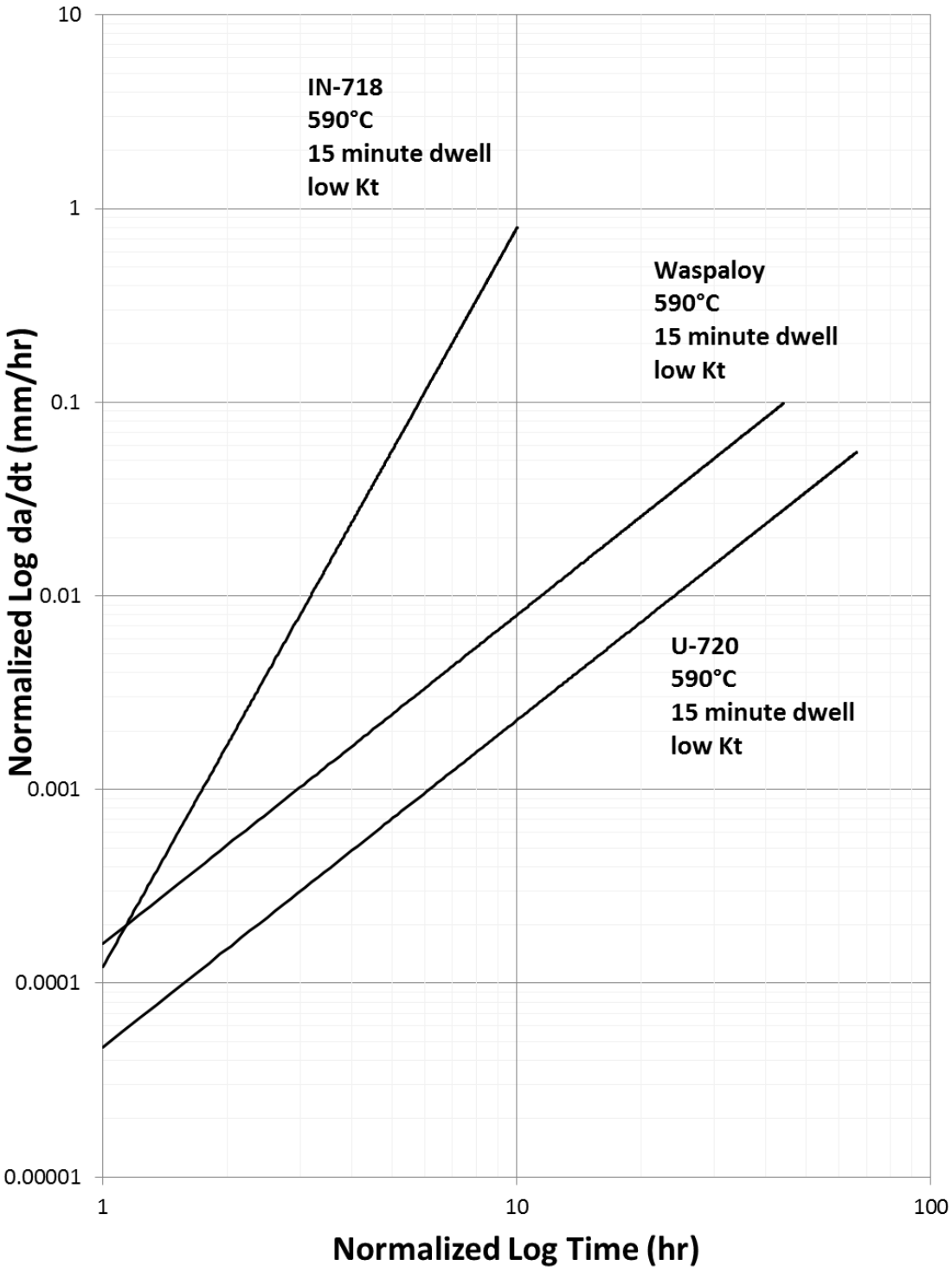

Figure 5.36 Plot of time dependent crack growth comparison of IN-718, U-720 and Waspaloy material (590 °C, low K_t, 15 minute dwell)

The slope of the crack growth curves indicates that the IN-718 material had a faster growth rate than Waspaloy or U-720. The slope of the crack growth curve has an asymptotic direction in comparison to the other two alloys. The U-720 material has the slowest crack growth rate. This is expected because the IN-718 material is the least temperature capable in comparison to the other two alloys.

5.6 Crack Tunneling

The the fracture surfaces were photographed using a Keyence DHX digital microscope. Calibrated surface measurements were applied to the fracture surface pictures in order to measure the crack length on the surface of the specimen in comparison to the crack length through the depth of the specimen. A minimum of two measurements were taken for both the surface and depth measurements in order to provide an average value for each. In order to determine the crack tunneling ratio, the two values were averaged and then subtracted to create a delta ratio. A summary of the crack tunneling measurements is provided in Table 5.1 for Waspaloy material, Table 5.2 for IN-718 material, and Table 5.3 for U-720 material.

Table 5.1 Summary of Crack Tunneling Measurements for IN-718 Material

Specimen Number	**Stress Concentration (K_t)**	**Temp (°C)**	**Average Surface Length (mm)**	**Average Depth Length (mm)**	**Crack Tunneling Ratio**
1	Low	540	2.97	3.00	0.108
2	Low	540	1.75	3.98	2.23
3	Low	590	2.49	3.58	1.09
4	High	540	2.86	2.51	0.349
5	High	540	2.82	3.68	0.864
6	High	540	2.60	2.64	0.603
7	Low	470	0.521	0.635	0.114
8	Low	540	0.572	1.21	0.635
9	Low	540	0.667	1.26	0.597
10	Low	590	0.743	2.80	2.06
11	Low	590	1.33	1.45	0.123

Table 5.2 Summary of Crack Tunneling Measurements for Waspaloy Material

Specimen Number	Stress Concentration (K_t)	Temp (°C)	Average Surface Length (mm)	Average Depth Length (mm)	Crack Tunneling Ratio
1	N/A	1000	2.93	3.37	0.432
2	N/A	1100	3.51	4.88	1.18
3	N/A	1200	2.96	6.04	3.08
4	Low	1100	1.14	2.96	1.82
5	Low	1000	0.527	0.508	0.019
6	Low	1100	0.286	0.419	0.133
7	Low	1100	1.35	2.74	1.40
8	Low	1000	2.07	2.71	0.635
9	Low	1200	1.35	3.111	1.76
10	Low	1200	1.23	3.22	1.88
11	Low	1200	0.98	2.32	1.35

Table 5.3 Summary of crack tunneling measurements for U-720 material

Specimen Number	Stress Concentration (K_t)	Temp (°C)	Average Surface Length (mm)	Average Depth Length (mm)	Crack Tunneling Ratio
1	Low	1100	2.67	3.56	0.883
2	Low	1200	1.62	2.51	0.895
3	Low	1200	1.84	3.52	1.676
4	High	1200	1.78	2.07	0.290
5	High	1200	1.97	2.37	0.398

Those specimens which had a ratio of greater than 1.0 were considered to show positive signs of crack tunneling. Those specimens which had a ratio of less than 0.5 did not show signs of crack tunneling. Those specimens which had a crack tunneling ratio between 0.5 and 1 show a potential transition point between non-tunneled and tunneling behavior. The stress concentration factor and test temperature were included in the tables above to demonstrate whether these parameters had a significant effect on the pre-disposition for crack tunneling to

occur. For IN-718, there was not a clear pattern between crack tunneling and a specific parameter such as dwell time, K_t, or test temperature. Waspaloy and U-720, on the other hand, had a clearer trend that the high temperature and low K_t specimens were more likely to experience crack tunneling.

Crack tunneling can appears in a variety of shapes on the fracture surface. An example of fracture surface that does show evidence of crack tunneling is shown in Figure 5.37. The irregular shape of the heat tinting visually demonstrates the constraints on the crack front as it moves across the cross section of the material.

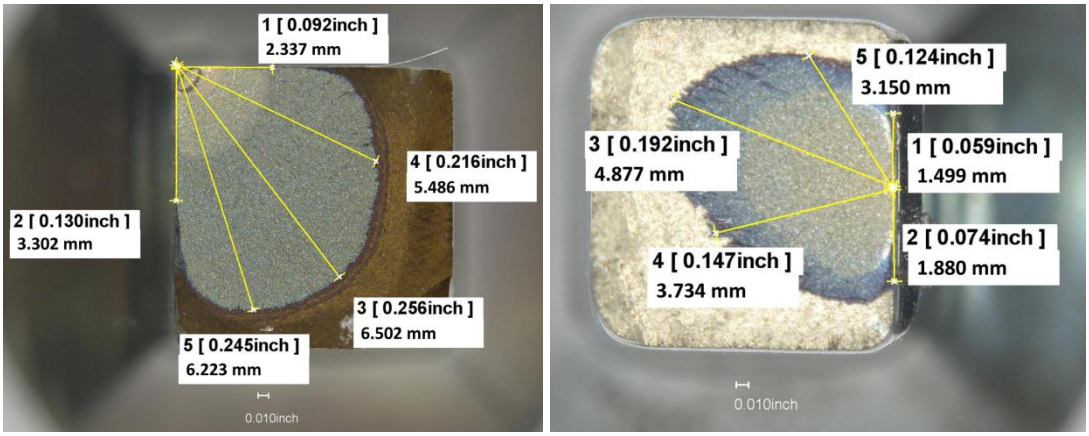

Figure 5.37 Examples of fracture surface which display evidence of crack tunneling

Those specimens which do not display signs of crack tunneling have a more uniform semi-circular crack front. This indicates less resistance to the crack growth moving across the specimen. An example of a fracture surface which does not show signs of crack tunneling is shown in Figure 5.38.

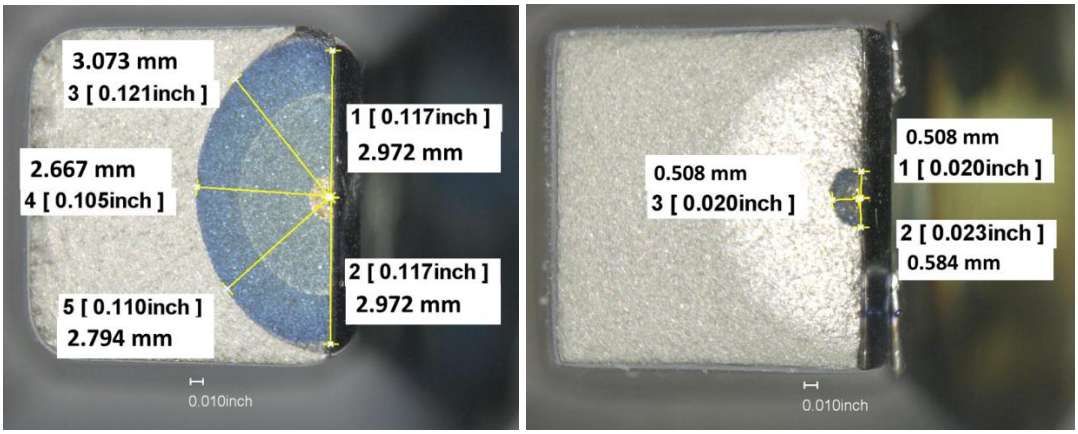

Figure 5.38 Examples of fracture surfaces which do not display evidence of crack tunneling

The colors on the fracture surface are from the heat tint operation to calibrate the crack length measurements from the DCPD system. The overall color indicates how much of the crack was exposed during the heat tint operation, but the color changes are not indicative of tunneling. The crack tunneling response will provide another indicator of transition. Those specimens which are either going through the transition from cycle dependent crack growth to an intermediate state or from an intermediate state to time dependent crack growth will show signs of crack tunneling. The goal would be to use this as a signal to the modeler that the crack growth model should be run with creep effects and crack tunneling effects included ensuring that the model is accurate.

CHAPTER 6. DISCUSSION

Microstructural fractography and crack front behavior are both clear signs of transition occurring in a material as it changes from a cycle dependent crack growth mechanism to a time dependent crack growth mechanism. The crack propagation results demonstrate which parameters have a more dominant effect on the growth rate. The fracture surfaces provide a clear perspective on the mechanism which controls the crack path.

The physical appearance of the fracture surface in this research program will validate the theories that go into the models. Environmental effects are expected to produce signs of cleavage while a material undergoes plastic deformation. During intergranular crack growth, the crack can move along several planes. This allows for the crack direction to change more frequently and increase the potential for secondary cracking in intergranular fracture. A ductile fracture surface can present itself as a series of dimples. Striations are a clear indicator of fatigue crack progression. Under crack blunting conditions, the striations will appear stretched right before failure occurs (Broek).

6.1 Creep Crack Growth

Creep crack growth resistance is much higher in air than in vacuum. Different alloys have a different level of resistance to environmental effects based on the microstructural structure and composition. For example IN-718 has been shown to be much more sensitive in comparison to other nickel base alloys. In typically fatigue crack growth, the crack tip sharpens on each load cycle; however under creep conditions, the crack tip has a tendency to blunt with subsequent load and time (Shahinian & Sadanada, 1989).

The mechanisms acting in creep crack growth suggest that dislocations will build up at the crack tip to block crack propagation. The IN-718 results validate this theory, the dwell crack growth testing experienced a faster growth rate relative to the creep growth rate. The Waspaloy material data, on the other hand, indicates that the growth rate increased as the dwell time increased. The Waspaloy creep crack growth had the fastest growth rate. This could indicate that the Waspaloy experienced crack retardation during dwell testing while the IN-718 did not. The Waspaloy crack growth test data indicated that the 60 minute dwell specimens had a faster growth rate that the 15 minute dwell specimens. This indicates that a greater amount of crack tip blunting and crack retardation occurred during the 15 minute dwell period. At the high temperature condition, the Waspaloy material saw an increase in growth rate with increasing dwell time.

The creep crack growth testing did not see a slope change at high time testing which is associated with environmental effects and crack retardation. This slope change was present in the dwell crack growth testing, especially in the Waspaloy material. Shahinian and Sadanada posited that a static load condition would see more oxidation effects than cyclic testing and therefore experience more crack tip blunting and retardation (Shahinian & Sadanada, 1989). The test results documented here suggest that this theory is inaccurate or that a higher test temperature would be required to further activate oxidation and closure mechanisms under the creep condition and see evidence of retardation effects.

The fracture surfaces of the creep crack growth specimens indicate that the creep condition does cause the material to behave in a time-dependent fashion. The creep crack growth specimens showed a clear switch from a transgranular pre-crack region to an intergranular growth pattern. Therefore, the creep crack growth does the increased crack growth rate as a part of the time dependent crack growth mechanism, but according to the crack growth data, it does not experience any subsequent decrease in crack growth as part of the environmental effects.

6.2 Time Dependent Crack Growth

The time dependent crack growth results demonstrates how the different dwell periods affect the crack growth rate and resulting fracture surface morphology. The Waspaloy test results indicate that long dwell periods lead to a faster crack growth rate. This response demonstrates the influence of environmental effects and the oxidation based retardation mechanism. At longer dwell periods, the crack surface is exposed to the air environment for longer periods of time. This allows for both the oxide layer to develop on the surface and for addition oxygen to diffuse into grain boundaries. The crack tip opening displacement can be affected by oxygen diffusion causing a closure mechanism. Crack closure mechanisms were used by Newman to explain test data patterns. In threshold testing, oxide accumulation can cause a knee shape to appear in the test data representative of crack closure (Newman, 1999). Crack retardation is cause by plasticity acting behind the crack tip. The crack is forced to propagate through the regions which had experienced previous plastic deformation motion and is working to close the crack tip (Grandt, 2004). Therefore, it was expected that the crack growth rate would continuously increase with increasing dwell time, but that all three curves would experience crack growth retardation effects. Based on the diffusion theory, there should be a limit to the increase in growth rate associated with increased dwell time. The saturation limit forms the basis of the Maximum Growth Rate, the idea that there is a limit on how much the rate can increase based on diffusion limits.

The fracture surface results indicate that all Waspaloy dwell testing transitioned from a transgranular pre-crack region to an intergranular crack growth progression across the rest of the cross section. The majority of these dwell tests were compared at the maximum temperature for Waspaloy so it is consistent with the DOE strategy that all specimens would transition. In order to create conditions for transition, a lower load level or dwell time would be required.

6.3 Geometry

Stress concentration factors near the crack tip help further increase the amount of oxygen diffusivity by decreasing the amount of activation energy required for diffusion to occur (Zheng & Ghonem, Part II, 1991). Two different geometries were evaluated in this study to evaluate the effect on the crack propagation rate and the resulting fracture surface morphology. The IN-718 data shows very little difference between the crack growth rate at low and high K_t values. The U-720 test results also showed little difference between the two different notch geometries. This indicates that a different test parameter, such as temperature, had a more dominant effect on the crack growth rate than the notch geometry. The Waspaloy test results indicate that the crack growth rate increases at the K_t factor increases. The crack growth rate data suggests that the rate increases slightly as the notch K_t factor increases. The stress concentration factor or K_t acts to focus the stress. Any increase in the K_t factor indicates a larger notch which will act to localize the stress levels more than a smaller K_t value on the surface of a test specimen.

The stress concentration factor controls the shape of the plastic zone and the dislocation emission pattern. A high stress concentration factor focuses the dislocations within a smaller plastic zone which acts to increase the crack growth rate rather than allowing the dislocations to diffusion over a larger plastic zone at a low stress concentration factor. With a smaller plastic zone, the applied load is acting on a smaller portion of the specimen cross section, instead of being distributed across the entire cross section, making it easier for the crack growth rate to increase. An illustration of the stress concentration factor and resulting plastic zone is shown in Figure 6.1.

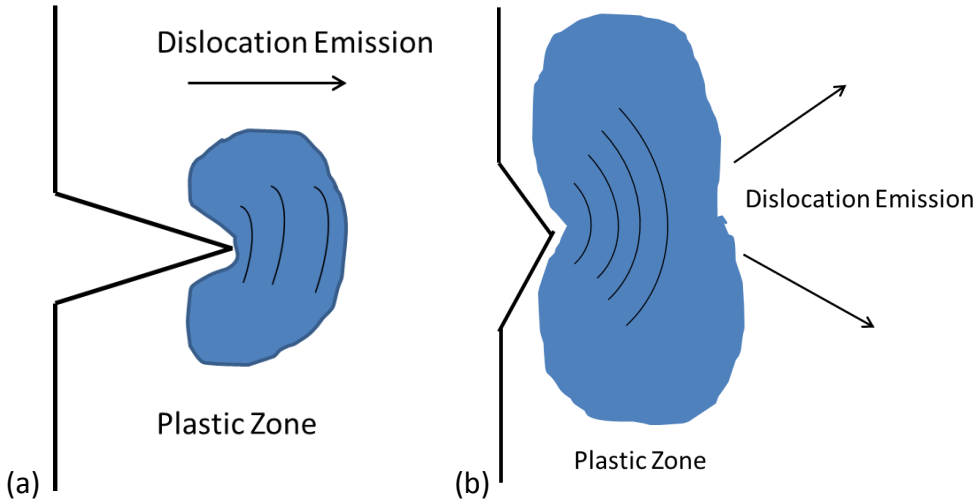

Figure 6.1 An illustration of the effect of the stress concentration factor on the plastic zone size and dislocation motion: (a) high K_t condition, (b) low K_t condition

The effect of the stress concentration factor will decrease as the crack tip moves from the surface near the machined K_t to the center of the specimen. Once the crack tip is no longer influenced by the geometry, the plastic zone will return to a bulk response which should have more homogeneous stress concentrations.

The fracture surfaces of the geometry test specimens had a varied response based on the material and the temperature. For the IN-718 and Waspaloy specimens, the low K_t specimens demonstrated a mixed mode crack growth response. The high K_t specimens, on the other hand, showed a clear transition from a transgranular pre-crack to an intergranular crack path. This suggests that the low K_t geometry does not focus the stress enough to cause transition, while the high K_t geometry causes enough stress localization to force the crack to switch to intergranular growth. The U-720 specimens both showed a clear transition from a transgranular pre-crack to an intergranular crack path across both specimens. This is expected since they did not show a large difference in the crack propagation data.

6.4 Temperature

At high temperatures, one of the primary concerns is the amount of oxidation which can alter the material behavior based on grain boundary embrittlement. Experimental work by Krupp et al showed that high temperature testing saw the most oxidation diffusion while the lower temperature testing was driven more by preferential and limited diffusion. The limitations on the amount of grain boundary diffusivity also depend on the structure of the grain boundaries in a particular material (Krupp, Kane, Pfaendtner, Liu, Laird, & McMahon, 2004). There is a maximum rate and saturation limit for oxygen diffusion which can limit the overall oxidation level. This oxidation limit can contribute to the Maximum Growth Rate Theory which assumes that there is a limit to the amount of crack growth acceleration from environmental effects (Zheng & Ghonem, Part II, 1991).

Three different temperatures were tested on the IN-718 material. The goal was to target a temperature range above and below the predicted dwell transition temperature along with a mid-point temperature to assist with data interpolation. The IN-718 crack propagation results indicate that the crack growth rate increases with increasing temperature. Again there are only minor differences between low and high level loading at the same temperature, so the temperature is a larger driving force in comparison to the load levels or geometry based on the results from low and high K_t testing.

The fracture surface morphology at all three temperatures displayed characteristics consistent with mixed mode transition. The low temperature testing is primarily transgranular. The medium and high temperature testing has a transition between the transgranular pre-crack and the intergranular crack growth; however, there are transgranular crack growth features embedded in the intergranular region. While temperature seems to be the greatest driving force for IN-718 material to alter the crack growth rate, the fracture surface does not reflect the same changes.

Some crack growth research has focused on processing nickel material in new ways to control the amount of grain boundary oxidation that occurs and increases the crack growth rate. Krupp suggested that repetitive mechanical working and stress relieving heat treatments could increase the material resistance to crack propagation. Within an alloy there are preferential grain boundaries, some of those grain boundaries help enable diffusion across the grain boundaries while other directions delay diffusion. Deformation processing can increase the population of grain boundaries which delay diffusion, these are sometimes called Coincidence-Site Lattices or CSLs. Cold rolled IN718 test specimens underwent this type of processing which has increased the fracture resistance of the material. The processed specimens showed increased incubation time before evidence of cracking occurred in comparison to the non-processed specimens (Krupp, Kane, Liu, Dueber, Laird, & McMahon, 2003). This type of processing could improve the capability of the IN-718 material test here and potentially have beneficial effects on the Waspaloy and U-720 material as well.

6.5 Load Sequence

As described above, the one of the Waspaloy specimens was tested under two different types of waveforms to re-sharpen the blunted crack growth tip between dwell cycle periods. The transition between the three each type of waveform has a clear delineation point that demonstrates how the dwell cycle cause the switch from cycle dependent to time dependent crack growth behavior. Under the original dwell cycle the Waspaloy material transitioned from a transgranular pre-crack to an intergranular crack while the dwell waveform was applied. Then the dwell waveform was replaced with a triangular waveform, the material transitioned back to a transgranular path until the dwell was reapplied.

This type of low sequence could represent a break in a cruise cycle. For example, if an airplane performed a mid-flight altitude change to avoid turbulence, the load cycle might be interrupted. These results indicate that the interruption

could increase the effects of time dependent crack growth by allowing the crack tip to re-sharpen. The crack growth data does not indicate that any crack retardation occurs; this is attributed to the re-sharpening period where the crack tip blunting is prevented by the applied waveform.

As predicted, the overload mission cycle cause retardation which is visible in the crack propagation rate data. There were two types of overload conditions which were tested as a part of this research program. The first condition is an overload level of 105% of the maximum dwell load condition. The crack propagation data for this test was compared against a standard dwell fatigue crack growth test cycle at the same parameters. The low temperature test results show a large amount of retardation in the overload data. There was not an appreciable difference between the low overload and high overload test data, but both demonstrate retardation compared to the standard dwell crack growth test. The fracture surface demonstrates that the overload specimens have an intergranular crack path for a set period of time before the dwell effects relax out and the crack path returns to a transgranular progression. The high load applied during the overload period ensures that there is enough oxidation present to cause intergranular crack growth, but the load also produces more dislocations during a short time period which can cause dislocation shielding and crack tip blunting. If the crack tip experiences enough resistance, it may return to a transgranular crack path and cycle dependent behavior. The fracture surface of the low temperature overload testing is an example where competing crack growth mechanisms can change the overall crack growth cycle.

The high temperature test results, on the other hand, show that there is little difference between the dwell propagation data and the low overload data. This response indicates that the low overload level is not enough to cause crack retardation and change the crack propagation rate. The fracture surface for this test indicated that there was a transgranular growth region for the pre-crack and overload region and then the growth transitioned to the intergranular region to accompany the dwell crack growth segment of the mission. There was no

perceptible difference between the transgranular pre-crack region and the overload transgranular region. The second overload condition tested was a higher overload level. The high overload profile was approximately 120% of the maximum dwell cycle load level. These same test results were also compared to standard dwell testing. In contrast to the low overload level testing, the crack propagation results for the high overload testing show that crack retardation effects are present and that there is a decrease in the overall propagation rate. The fracture surface morphology indicated that there was a transgranular pre-crack region followed by a more violent transgranular region that accompanied the overload period. Intergranular crack propagation was evident for the dwell crack growth region.

Crack retardation after an overload is a result of plasticity induced closure referred to as the Elber Mechanism (Schjive, 2001). The test results confirm that the overload level must be high enough to cause crack retardation. The low level overload cycle was not enough to cause crack retardation while the high overload level did cause a change in the crack propagation rate. The fracture surface morphology also confirms that a change is occurring in the material. Both overload cycles occurred in a transgranular crack growth pattern, but the high overload level did have evidence of a more violent crack path.

Test frequency can have a large impact on the impact from loading. This program did not get the opportunity to isolate frequency as one of the test parameters in the mechanism map. This is something that could be applied to future testing to improve upon these results.

6.6 Material

The three alloys which were evaluated in this research program were expected to perform in a similar pattern based on their composition and grain structure. The microstructure evaluation confirmed this expectation and demonstrated that there are only minor changes in grain size across the specimen population. A comparison

of the growth rates suggests that the crack propagation in IN-718 is much faster than Waspaloy or U-720 material which had a similar slope. The fracture surfaces also indicate that the U-720 and Waspaloy material were more likely to transition to a fully intergranular crack path at a variety of test conditions. This indicates that IN-718 has some competing mechanisms which prevent the material from experiencing crack retardation and time-dependent microstructural effects. This could also suggest that IN-718 has a wider transitional region between cycle-dependent and time-dependent crack growth, whereas the transition region for Waspaloy and U-720 may be much smaller.

6.7 Crack Tunneling

The crack tunneling response was varied across the three materials. Evidence of crack tunneling is most commonly observed in threshold crack growth testing and in time dependent crack growth testing with a dwell (VanStone, Gooden, & Krueger, 1988). The crack tunneling ratio measurements indicate that the surface examination of the fracture surface can provide a definitive perspective on whether or not crack tunneling is present in a crack growth specimen. A visual examination compared to the measured ratio showed correlation between the results. As mentioned above, all specimens which had a ratio from 0 to 0.05 did not show evidence of crack tunneling. All specimens which had a ratio greater than 1.0 did show evidence of tunneling. Those specimens that have a ratio greater than 0.5 but less than 1.0 were in a transitional period between tunneling and not tunneling.

Crack tunneling does not correlate directly to time dependent or cycle dependent crack growth. Those specimens which are consistently transgranular or consistently intergranular typically do not show signs of crack tunneling. Those specimens which show signs of crack tunneling are indicative of a transitional period, such as those specimens which transition from transgranular to intergranular specimens or those which display mixed mode fracture surface characteristics. Crack tunneling can be used as a visual cue of that transitional state.

Crack tunneling is caused by the build-up of an oxide layer on the surface of the material after exposure to an air environment at elevated temperatures. At the surface, the oxide layer can create more barriers to crack propagation via grain boundary embrittlement. Based on the diffusion condition, it can take additional time and energy for grain boundary embrittlement to occur sub-surface. For those specimens which experience fully intergranular crack propagation, it would indicate that the material is fully saturated in terms of oxidation effects so that crack growth would be the same on the surface as well as into the depth. However, for a material that is in transition would see the limitation on the surface prior to the limitation which would occur below the surface. The IN-718 test specimens did not seem to have a correlation between the test parameters and the resulting levels of crack tunneling. The Waspaloy and U-720 specimens had high crack tunneling ratios at high temperature and a low K_t geometry. The temperature could increase the amount of oxygen diffusion and block the crack along the surface. The low K_t geometry may change the plastic zone shape enough to alter the crack progression both through the material and on the surface.

Crack models can account for the predisposition towards crack tunneling. The crack pattern on the surface versus the depth of cross section can significantly affect how the crack propagates and when a component might fail in an engine application. Those specimens which display evidence of crack tunneling are the most eligible candidates for advanced time dependent crack growth modeling. Crack tunneling operates as a macroscopic physical indicator of the start of transition and works with SEM analysis to determine which mechanisms are operating at a certain set of conditions.

6.8 Mechanism Map Summary

In order to compile the results, the simplified mechanism map was updated with the parameters tested above to indicate approximate locations on the map where transition should occur. As predicted the low temperature and low load

specimens are well within the transition zone between cycle dependent and time dependent crack growth regimes. As the temperature, load, and geometry increases the crack growth results are closer towards the fully time dependent crack growth regime. The mechanism map is shown in Figure 6.2.

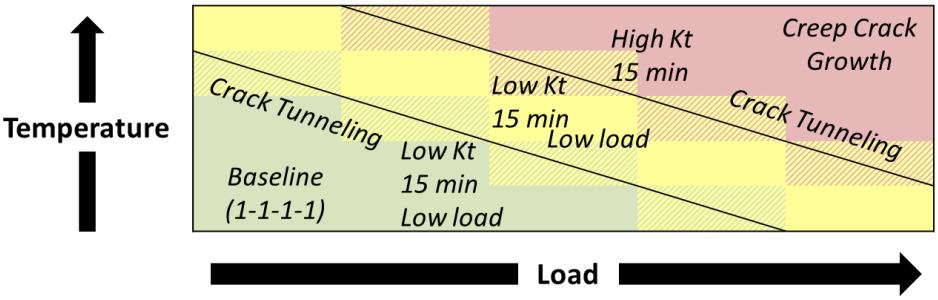

Figure 6.2 IN-718 mechanism map summary

All three materials showed slightly different variations on this mechanism map. The IN-718 testing had more specimens in the transitional mixed mode region while Waspaloy material had fewer specimens which would be considered transitional results. This indicates that the IN-718 transitional region is well documented to order to calibrate the modeling approach. The Waspaloy, on the other hand may require additional characterization to locate the transition conditions. This indicates that lower stress and temperature increments would be required to locate the transition conditions, or that the margin between the cycle dependent and time dependent regime is so small that it would be very difficult to target a set of conditions to achieve transition.

CHAPTER 7. CONCLUSIONS & RECOMMENDATIONS

Time dependent fatigue crack growth has very distinct physical characteristics and a discernable effect on the crack growth rate of a material. While the traditional time dependent crack growth models only relied on temperature for transition, this research program included several additional factors including geometry, load sequence, and load levels to increase the efficacy of the models at the intermediate levels of the mechanism map. While the modeling process itself is documented via the patented process, this work demonstrates the physical concept related to transition and transition mechanisms. Isolated comparisons were made across three different nickel base super alloys to identify which extrinsic mechanisms create a driving force for the crack growth behavior.

The geometry comparison demonstrated that a high stress concentration factor increases the propensity for the material to transition from cycle dependent to time dependent crack growth. This response was consistent across the two alloys tested.

The load level and load cycle also have a significant effect on the transition properties. Low and high loads were tested for several conditions, but the relative load levels did not seem to have as much as an effect as the other factors which were varied during the test program. The load sequence; however, caused crack retardation to occur when the overload cycle was impose with a high enough load level prior to the dwell period. The application of a high load by itself is not enough to change crack growth behavior, but the combination of high load levels with an overload cycle can change the crack growth mechanism.

The environment and temperature of a component cause time dependent fatigue crack growth behavior. While elevated temperature is a well-known contributor to the time dependent mechanism, there is limited research on creep crack growth in comparison the dwell crack growth. The crack growth rate data indicates that the creep crack growth data follows the same trend as dwell crack growth data, except that the dwell crack growth data shows more evidence of crack retardation compared to the creep crack data. All tests were performed in air, so the crack growth rates and fracture surface morphology are all a result of the environmentally assisted mechanisms. While there is some change in crack growth rate under different temperatures and loading, there appears to be a maximum growth rate level that could be associated with the maximum amount of oxygen diffusion which can occur in a material.

Transitional results are those conditions which were not fully cycle dependent or fully time dependent. Those specimens display evidence of competing mechanisms which can the fracture surface appearance and highlight the reason for the more advanced models. Crack tunneling measurements support the transitional regions by demonstrating the visible constraints on the crack growth progression. The surface crack growth is limited by the oxidation effects while the sub-surface crack growth has more freedom to propagate. Those specimens which were fully transgranular or fully intergranular did not display evidence of crack tunneling.

The crack growth data and physical results documented here will be implemented into the proposed patent model to further refine the predictions and way that the model is applied to a variety of component-based inputs. While many conditions were captured by this test program, there is an opportunity for future testing to increase the sensitivity of the DOE and predicative capability of the model. Recommended future work includes additional focus on the change in crack growth behavior based on a variety of grain size and heat treatments to improve crack growth resistance. Additionally, it would be helpful to analyze a greater variety of test frequencies to confirm whether frequency is a dominant factor in the transition.

REFERENCES

REFERENCES

AMS 5663. (2009). Resistant, Bars, Forgings, and Rings 52.5Ni - 19Cr - 3.0Mb - 5.1Cb (Nb) - 0.90Ti - 0.50Al - 18Fe Consumable Electrode or Vacuum Induction Melted 1775 Degree F Solution and Precipitation Heat Treated. *Aerospace Material Specification*.

AMS 5704. (2009). Nickel Alloy, Corrosion and Heat Resistantm Forgings 57Ni - 19.5Cr - 13.5Co - 4.3Mo - 3.0Ti - 1.4Al - 0.05Zr - 0.006B Consumable Electrode or Vacuum Induction Melted 1825 to 1900 Degree F Solution Stabilization and Precipitation Heat Treated. *Aerospace Material Specification*.

Andersson, H., Persson, C., & Hansson, T. (2001). Crack Growth in IN718 at High Temperature. *International Journal of Fatigue, 23*, 817-827.

Andrieu, E., & Molins, R. (1992). Intergranular Crack Tip Oxidation Mechanism in a Nickel-based Superalloy. *Material Science and Engineering, A154*, 21-28.

Askeland, D., & Fulay, P. (2005). *The Science and Engineering of Materials.* Cengage Learning.

ASTME1457. (2013). Standard Test Method for Measurement of Creep Crack Growth Times and Rates in Metals. (A. S. Materials, Ed.)

ASTME2760. (2010). Standard Test Method for Creep-Fatigue Crack Growth Testing . (A. S. Materials, Ed.)

ASTME647-00. (2001). Standard Test Method for Measurement of Fatigue Crack Growth Rates. *American Society of Testing and Materials*.

Bache, M. R., Jones, J. P., Drew, G. L., Hardy, M. C., & Fox, N. (2009). Environment and Time Dependent Effects on the Fatigue Response of an Advanced Nickel Based Superalloys. *International Journal of Fatigue, 31*, 1719-1723.

Barker, V. M., Johnson, W. S., Adair, B. S., Antolovich, S. D., & Staroselsky, A. (2013). Load and Temperature Interaction Modeling of Fatigue Crack Growth in a Ni-base Superalloy. *International Journal of Fatigue, 52*, 95-105.

Beltz, G. E., Lipkin, D. M., & Fischer, L. (1977, May). Role of Crack Blunting in Ductile versus Brittle Response of Crystalline Materials. *Physical Review Letters, 82*(22), 4468-4471.

Boman, P.-O. K. (1992). *A Numerical Study of Crack Tip Blunting Under Cyclic Loading.* Massachussets Institute of Technology, Cambridge.

Broek, D. (n.d.). *Some Contributions of Electron Fracography to the Theory of Fracture.* National Aerospace Laboratory NLR The Netherlands.

Budynas, R. G., & Nisbett, J. K. (2011). *Shigley's Mechanical Engineering Design, Ninth Edition.* New York: McCraw.

Callister, W. D., & Rethwisch, D. G. (2011). *Material Science and Engineering An Introduction* (8th ed.). Hoboken, New Jersey: Wiley Custom Learning Solutions.

Caton, M. J., & Jha, S. K. (2010). Small Fatigue Crack Growth and Failure Mode Transition in a Ni-base Superalloy at Elevated Temperature. *International Journal of Fatigue, 32*, 1461-1472.

Cleri, F., Yip, S., Wolf, S., & Phillpot, S. (1997, August 18). Atomic-Scale Mechanism of Crack-Tip Plasticity: dislocation nucleation and crack-tip shielding. *Physical Review Letters, 79*(7), 1309-1312.

Columbus, D., & Grujicic, M. (2001). A Comparison of Mode I Fracture Behavior of FCC and BCC Metallic Materials: a discrete dislocation analysis. *Applied Surface Science, 180*, 138-161.

Connolley, T., Reed, P., & Starink, M. (2003). Short Crack Initiation and Growth at 600C in Notched Specimens of Inconel 718. *Material Science and Engineering, 340*(1-2), 139-154.

Dugdale, D. (1960). Yielding of Steel Sheets Containing Slits. *Journal of Mechanics and Physics of Solids, 8*, 100-104.

Evans, W. J. (2004). Time Dependent Effects in Fatigue of Titanium and Nickel Alloys. *Fatigue Fracture Engineering Material Structure, 27*, 543-557.

Frank, F. C., & Read, W. T. (1950, August 15). Multiplication Processed for Slow Moving Dislocations. *Physical Review*, 722.

Grandt, A. F. (2004). *Fundamentals of Structural Integrity: damage tolerant design and non-destructive evaluation.* Hoboken, New Jersey: John Wiley and Sons, Inc.

Hoshide, T., & Socie, D. F. (1987). Mechanics of Mixed Mode Small Fatigue Crack Growth. *Engineering Fracture Mechanics, 26*(4), 841-850.

Jahed, H., & Varvani-Farahani, A. (2006). Upper and Lower Fatigue Life Limites Model Using Energy-based Fatigue Properties. *International Journal of Fatigue, 28*, 467-473.

Krupp, Kane, W. M., Liu, X., Dueber, O., Laird, C., & McMahon, C. (2003). The Effect of Grain-Boundary-Engineering-Type Processing on Oxygen Induced Cracking of IN718. *Material Science and Engineering, A349*, 213-217.

Krupp, Kane, W., Pfaendtner, J., Liu, X., Laird, C., & McMahon, C. J. (2004). Oxygen-Induced Intergranular Fracture of the Nickel Base Alloy IN718 during Mechanical Loading at High Temperature. *Materials Research, 7*(1), 35-41.

Krupp, U., Wagenhuber, P., Jacobs, T., & McMahon, C. J. (2005). 5249-Environmentally Assisted Brittle Fracture of Nickel-Base Superalloys at High Temperatures. *ICF11.* Italy.

Mills, D. (2014). *Patent No. RCA 11191, 27163-227694.* United States of America.

Morrison, D. J., Chopra, V., & Jones, J. W. (1991). Effects of Grain Size on Cyclic Strain Localization in Polycrystalline Nickel. *Scripta Metallurgica et Materialia, 25*, 1299-1304.

Newman, J. (1999, April). Effects of Grain Size on Cyclic Strain Localization in Polycrystalline Nickel.

Noda, N., & Takase, Y. (1999). Stress concentration formulae useful for any shape of notch test specimen under tension and under bending. *Fatigue Fracture Engineering Material Structure, 22*, 1071-1082.

Pang, H. T., & Reed, P. (2003). Fatigue Crack Initiation and Short Crack Growth in Nickel-Base Turbine Disk Alloys - the effect of microstructure and operating parameters. *International Journal of Fatigue, 25*, 1089-1099.

Prakash, D., Walsh, M. J., Maclachan, D., & Kcrunsky, A. M. (2009). Crack Growth in Micro-mechanisms in the IN718 Alloy Under the Combined Influence of Fatigue, Creep and Oxidation. *International Journal of Fatigue, 31*, 1966-1977.

Reed, P., & King, J. (1992). Mixed Mode Fatigue Effects in Ni-base Single Crystals - Preliminary Results. *Scripta Metallurgica et Materialia, 26*, 1829-1834.

Reed, R. C. (2006). *The Superalloys: Fundamentals and Applications.* Cambridge: Cambridge University Press.

Riedel, H. (1977). A Dugdale Model for Crack Opening and Crack Growth under Creep Conditions. *Material Science and Engineering, 30*, 187-196.

Ritchie, R. O. (1999). Mechanisms of Fatigue Crack Propagation in Ductile and Brittle Solids. *International Journal of Fatigue, 100*, 55-83.

Schjive, J. (2001). *Fatigue of Structures and Materials.* London: Kluwer Academic Publishers.

Shahinian, P., & Sadanada, K. (1989). Creep and Fatigue Crack Growth Behavior in Some Cast Nickel-base Alloys. *Materials Science and Engineering, A108*, 131-140.

Tong, J., Dalby, S., Byrne, J., Henderson, M., & Hardy, M. (2001). Creep, fatigue and oxidation in crack growth in advanced nickel base superalloys. *International Journal of Fatigue, 23*, 897-902.

VanStone, R., Gooden, O., & Krueger, D. (1988). *Advanced Cumulative Damage Modeling.* AFWAL-TR-88-4146: Air Force Research Group.

Vitek, V. (1977, February). A Theory of the Initiation of Creep Crack Growth. *International Journal of Fracture, 13*(1), 39-50.

Vitek, V. (1978). *Acta Metallurgica, 26*, 1345-1356.

Wanhill, R. J. (1999, September). Significance of Dwell Cracking for IN718 Turbine Disks.

Weerasooriya, T. (1987, June). Effect of Frequency in Fatigue Crack Growth Rate of Inconel 718 at High Temperature.

Zheng, D., & Ghonem, H. (1991). Part I. *Fatigue Fracture Engineering Material Structure, 14*(7), 749-760.

Zheng, D., & Ghonem, H. (1991). Part II. *Fatigue Fracture Engineering Material Structure, 14*(7), 761-768.

Zheng, D., Rosenberger, A., & Ghonem, H. (1993). Influence of pre-straining on high temperature, low frequency fatigue crack growth in superalloys. *Material Science and Engineering, A161*, 13-21.

APPENDIX

APPENDIX. FULL TEST MATRIX

The summary of the experimental methods provided individual comparisons of specific examples from the test program. Below is a summary of the full set of test conditions for reference. Those specimens which were tested but did not completely fracture and break open during the test sequence are labeled “NOT BROKEN.” Those specimens were assumed to have limited crack growth levels and could not significantly contribute to the physical evidence for transition.

Table A-7.1 IN-718 Full Test Matrix

Specimen Type	Specimen Number	Temperature (°C)	Dwell Time	K_t	Fracture Type *	Crack Tunneling
CT	1	537.8	N/A	N/A	Inter	N/A
CT	2	593.3	N/A	N/A	Inter	N/A
CT	3	468.3	N/A	N/A	Inter	N/A
RLH10042 mod 1	1	537.8	N/A	Low	Trans	No
RLH10042 mod 1	13	537.8	N/A	Low	NOT BROKEN	
RLH10042 mod 1	2	537.8	15 min	Low	Mixed Mode	Yes
RLH10042 mod 1	3	537.8	15 min	Low	NOT BROKEN	
RLH10042 mod 1	4	593.3	15 min	Low	Inter	Yes
RLH10042 mod 1	5	593.3	15 min	Low	NOT BROKEN	
RLH10042 mod 1	6	468.3	15 min	Low	NOT BROKEN	
RLH10042 mod 1	7	468.3	15 min	Low	NOT BROKEN	
RLH10042 mod 2	14	537.8	15 min	High	Inter	Transition
RLH10042 mod 2	15	537.8	15 min	High	Inter	No
RLH10042 mod 1	17	468.3	15 min	Low	Inter	No
RLH10042 mod 1	19	537.8	15 min	Low	Inter	Transition
RLH10042 mod 1	20	537.8	15 min	Low	Inter	Transition
RLH10042 mod 1	22	593.3	15 min	Low	Inter	Yes
RLH10042 mod 1	23	593.3	15 min	Low	Inter	No
RLH10042 mod 1	25	593.3	15 min	Low	NOT BROKEN	

*trans = transgranular, inter = intergranular

Table A-7.2 Waspaloy Full Test Matrix

Specimen Type	Specimen Number	Temperature (°C)	Dwell Time	K_t	Fracture Type *	Crack Tunneling
CT	1	538.9	N/A	N/A	Inter	N/A
CT	2	593.3	N/A	N/A	Inter	N/A
CT	3	648.9	N/A	N/A	Inter	N/A
RLH10042	1	538.8	15 min	N/A	Inter	No
RLH10042	2	593.3	15 min	N/A	Inter	Yes
RLH10042	3	648.9	15 min	N/A	Inter	Yes
RLH10042 mod 1	2	593.3	15 min	Low	Inter	Yes
RLH10042 mod 1	3	537.8	15 min	Low	Mixed Mode	No
RLH10042 mod 1	4	537.8	15 min	Low	Mixed Mode	No
RLH10042 mod 1	5	593.3	60 min	Low	NOT BROKEN	
RLH10042 mod 1	6	593.3	60 min	Low	Inter	Yes
RLH10042 mod 1	7	537.8	60 min	Low	Inter	Transition
RLH10042 mod 1	8	537.8	60 min	Low	NOT BROKEN	
RLH10042 mod 1	9	648.9	15 min	Low	NOT BROKEN	
RLH10042 mod 1	10	648.9	15 min	Low	Inter	Yes
RLH10042 mod 1	11	648.9	5 min	Low	Inter	Yes
RLH10042 mod 1	12	648.9	60 min	Low	Inter	Yes
RLH10042 mod 2	1	537.8	5 min	High	NOT BROKEN	
RLH10042 mod 2	2	593.3	15 min	High	NOT BROKEN	
RLH10042 mod 2	3	648.9	60 min	High	NOT BROKEN	
RLH10042 mod 2	4	537.8	15 min	High	Inter	No

*trans = transgranular, inter = intergranular

Table A-7.3 U-720 Full Test Matrix

Specimen Type	Specimen Number	Temperature (°C)	Dwell Time	Kt	Fracture Type*	Crack Tunneling
RLH10042 mod 1	1	537.8	15 min	Low	NOT BROKEN	
RLH10042 mod 1	2	593.3	15 min	Low	Inter	Transition
RLH10042 mod 1	3	648.9	15 min	Low	Inter	Transition
RLH10042 mod 1	4	648.9	15 min	Low	Inter	Yes
RLH10042 mod 1	5	648.9	15 min	Low	Inter	No
RLH10042 mod 2	6	648.9	15 min	Low	inter	No

*trans = transgranular, inter = intergranular